Obesity Impairs Short-Term and Working Memory through Gut Microbial Metabolism of Aromatic Amino Acids

Graphical Abstract
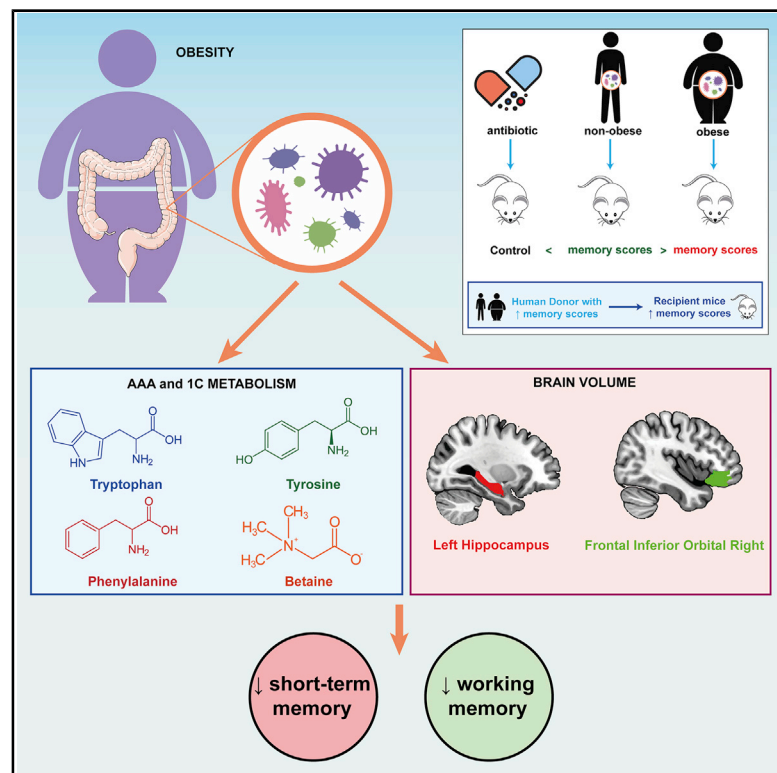
Authors

María Arnoriaga-Rodríguez,
Jordi Mayneris-Perxachs,
Aurelijus Burokas, ...,
Manuel Portero-Otin,
Rafael Maldonado,
José Manuel Fernández-Real

Correspondence

rafael.maldonado@upf.edu (R.M.),
jmfreal@idibgi.org (J.M.F.-R.)

In Brief

Learning and memory have recently been associated with specific microorganisms and metabolites. Here, Arnoriaga-Rodríguez et al. reveal a unique microbiota profile associated with memory through pathways involving aromatic amino acid and one-carbon metabolism. Importantly, these relationships are modulated by obesity; fecal microbiota transplantation from human subjects with obesity decreases the memory score of recipient mice.

Highlights

- Metagenomic data associate AAA and 1-C metabolism with memory and brain region volumes

- Memory scores are associated with altered plasma levels of AAA and betaine

- Obesity modulates these relationships and is associated with impaired memory

- FMTs from obese subjects lead to decreased memory scores in recipient mice

CellPress

Clinical and Translational Report

Obesity Impairs Short-Term and Working Memory through Gut Microbial Metabolism of Aromatic Amino Acids

María Arnoriaga-Rodríguez,[1,2,3,4,19] Jordi Mayneris-Perxachs,[1,2,3,19] Aurelijus Burokas,[5,18] Oren Contreras-Rodríguez,[2,6] Gerard Blasco,[7,8] Clàudia Coll,[9] Carles Biarnés,[7] Romina Miranda-Olivos,[2,6] Jèssica Latorre,[1,2,3] José-Maria Moreno-Navarrete,[1,2,3,4] Anna Castells-Nobau,[1,2,3] Mònica Sabater,[1,2,3] María Encarnación Palomo-Buitrago,[1,2] Josep Puig,[4,7,8] Salvador Pedraza,[4,8,10] Jordi Gich,[4,11] Vicente Pérez-Brocal,[12,13] Wifredo Ricart,[1,2,3,4] Andrés Moya,[12,13,14] Xavier Fernández-Real,[15] Lluís Ramió-Torrentà,[4,9,11] Reinald Pamplona,[16] Joaquim Sol,[16] Mariona Jové,[16] Manuel Portero-Otin,[16] Rafael Maldonado,[5,17,*] and José Manuel Fernández-Real[1,2,3,4,20,*]

[1]Department of Diabetes, Endocrinology and Nutrition, Dr. Josep Trueta University Hospital, Girona, Spain
[2]Nutrition, Eumetabolism and Health Group, Girona Biomedical Research Institute (IdibGi), Girona, Spain
[3]Biomedical Research Networking Center for Physiopathology of Obesity and Nutrition (CIBEROBN), Madrid, Spain
[4]Department of Medical Sciences, Faculty of Medicine, Girona University, Girona, Spain
[5]Laboratory of Neuropharmacology, Department of Experimental and Health Sciences, Universitat Pompeu Fabra, Barcelona, Spain
[6]Psychiatry Department, Bellvitge University Hospital, Bellvitge Biomedical Research Institute (IDIBELL) and CIBERSAM, Barcelona, Spain
[7]Institute of Diagnostic Imaging (IDI)-Research Unit (IDIR), Parc Sanitari Pere Virgili, Barcelona, Spain
[8]Medical Imaging, Girona Biomedical Research Institute (IdibGi), Girona, Spain
[9]Neuroimmunology and Multiple Sclerosis Unit, Department of Neurology, Dr. Josep Trueta University Hospital, Girona, Spain
[10]Department of Radiology, Dr. Josep Trueta University Hospital, Girona, Spain
[11]Girona Neurodegeneration and Neuroinflammation Group, Girona Biomedical Research Institute (IdibGi), Girona, Spain
[12]Department of Genomics and Health, Foundation for the Promotion of Health and Biomedical Research of Valencia Region (FISABIO-Public Health), Valencia, Spain
[13]Biomedical Research Networking Center for Epidemiology and Public Health (CIBERESP), Madrid, Spain
[14]Institute for Integrative Systems Biology (I2SysBio), University of Valencia and Spanish National Research Council (CSIC), Valencia, Spain
[15]Institute of Mathematics, École Polytechnique Fédérale de Lausanne (EPFL), Lausanne, Switzerland
[16]Metabolic Pathophysiology Research Group, Lleida Biomedical Research Institute (IRBLleida)-Universitat de Lleida, Lleida, Spain
[17]Hospital del Mar Medical Research Institute (IMIM), Barcelona, Spain
[18]Present address: Institute of Biochemistry, Life Sciences Center, Vilnius University, Vilnius, Lithuania
[19]These authors contributed equally
[20]Lead Contact
*Correspondence: rafael.maldonado@upf.edu (R.M.), jmfreal@idibgi.org (J.M.F.-R.)
https://doi.org/10.1016/j.cmet.2020.09.002

SUMMARY

The gut microbiome has been linked to fear extinction learning in animal models. Here, we aimed to explore the gut microbiome and memory domains according to obesity status. A specific microbiome profile associated with short-term memory, working memory, and the volume of the hippocampus and frontal regions of the brain differentially in human subjects with and without obesity. Plasma and fecal levels of aromatic amino acids, their catabolites, and vegetable-derived compounds were longitudinally associated with short-term and working memory. Functionally, microbiota transplantation from human subjects with obesity led to decreased memory scores in mice, aligning this trait from humans with that of recipient mice. RNA sequencing of the medial prefrontal cortex of mice revealed that short-term memory associated with aromatic amino acid pathways, inflammatory genes, and clusters of bacterial species. These results highlight the potential therapeutic value of targeting the gut microbiota for memory impairment, specifically in subjects with obesity.

INTRODUCTION

The decline of cognitive function is rising worldwide due to longer life expectancy (Larson et al., 2013) and increased preva-

lence of obesity and related metabolic disorders (Ward et al., 2019). Obesity has been identified as a modifiable risk factor for cognitive impairment (Kivipelto et al., 2018), but in turn, cognitive dysfunction is a predisposing factor for overeating and

Table 1. Clinical and Neuropsychological Data of the Human Discovery Cohort

	Total Population (n = 116)	Without Obesity (n = 51)	With Obesity (n = 65)	p
Age (years)	50.4 [41.8-58.5]	53.9 [44.4-59.0]	48.6 [41.1-57.1]	0.097
Females n (%)	81 (69.8)	34 (66.7)	47 (72.3)	0.511
Education (years)	12 [11-16.8]	15 [12-17]	12 [9-14]	9.0×10^{-6}
BMI (kg/m^2)	34.8 [25.3-43.3]	24.6 (2.6)	43.2 (6.7)	3.3×10^{-34}
Waist (cm)	110 [92-126]	89.8 (9.6)	125.2 (13.9)	3.6×10^{-29}
Fat mass (%)	43.6 [34-50.5]	32.4 (7.2)	49.9 (5.5)	2.7×10^{-27}
SBP (mmHg)	132.8 (20.0)	124.3 (15.8)	139.3 (20.6)	2.3×10^{-5}
DBL (mmHg)	74.8 (11.5)	71.2 (10.9)	77.6 (11.3)	0.003
HDL-C (mg/dL)	56 [45-68]	66.0 (17.0)	50.8 (12.7)	2.1×10^{-7}
Triglycerides (mg/dL)	90 [65.3-134.8]	79 [58-96]	123 [81.5-156]	7.1×10^{-5}
FPG (mg/dL)	96 [90-102.8]	95 [89-101]	97 [92.5-104.5]	0.196
HbA1c (%)	5.5 (0.3)	5.5 (0.3)	5.6 (0.3)	0.035
hsCRP (mg/dL)	2.4 [0.7-5.9]	0.7 [0.4-1.4]	5.0 [2.7-9.5]	8.1×10^{-14}
CVLT-IR (score)	61 [55-67.8]	65 [56-70]	59 [52.5-65]	0.003
CVLT-SDFR (score)	14 [12-15]	14 [12-16]	13 [11-14]	0.002
Total Digit Span (score)	14 [11.3-17]	15 [13-18]	13 [11-16]	0.003
PHQ-9 (score)	5.5 [3-9]	4 [2-6]	7 [4-10]	1.8×10^{-4}

Results are expressed as number and frequencies for categorical variables, mean and standard deviation (SD) for normal distributed continuous variables, and median and interquartile range [IQ] for non-normal distributed continuous variables. To determine differences between study groups, we used χ2 for categorical variables, unpaired Student's t test in normal quantitative, and Mann-Whitney U test for non-normal quantitative variables. p values for the difference between subjects with obesity (BMI > 30 kg/m^2) and without obesity (BMI between 18.5–30 kg/m^2). SBP, systolic blood pressure; DBP, diastolic blood pressure; HDL-C, high density lipoprotein cholesterol; FPG, fasting plasma glucose; HbA1c, glycated hemoglobin; hsCRP, high-sensitive C-reactive protein; CVLT, California Verbal Learning Test; IR, Immediate Recall; SDFR, Short Delayed Free Recall; PHQ-9, Patient Health Questionnaire.

obesity (Gunstad et al., 2020). One of the core cognitive domains that is impaired first is learning and memory (Petersen et al., 1999). Subjects with obesity have shown memory deficits, with body mass index (BMI) being negatively associated with memory traits across adult lifespan (Cournot et al., 2006; Gunstad et al., 2006).

The link between obesity and altered gut microbiota is clearly recognized (Ley et al., 2006). Increasing evidence supports the role of microbiota in cognitive disorders (Rogers et al., 2016; Sarkar et al., 2018). Learning and memory have been associated with specific microorganisms and metabolites (Mao et al., 2020). For example, the lack of microbiota produced fear extinction learning deficits in germ-free mice (Chu et al., 2019) and the administration of *Lactobacillus helveticus* prevented the memory impairment induced by a western diet (Ohland et al., 2013). *Bifidobacterium longum* also led to a beneficial effect in the object recognition tasks (Savignac et al., 2015). However, it is important to note that all of these studies have been performed in mice.

Evidence in humans is still scarce. Preliminary findings have shown impaired cognitive traits and detrimental metabolic profiles linked to some bacterial families in subjects with obesity (Arnoriaga-Rodríguez and Fernández-Real, 2019; Blasco et al., 2017; Fernandez-Real et al., 2015; Palomo-Buitrago et al., 2019). In fact, interventions that delay or prevent cognitive impairment, such as weight loss and treatment with some antidiabetic drugs, are well known to be associated with microbiota shifts (Brunkwall and Orho-Melander, 2017; Livingston et al., 2017; Maruvada et al., 2017).

Herein, we hypothesized that memory impairment is associated with both obesity status and a specific gut microbiome profile. We evaluated brain structure (through magnetic resonance imaging [MRI]) and function (using validated neuropsychological tests) in subjects with and without obesity and determined how these measurements associated with the gut microbiota and the plasma and fecal metabolome. We also tested whether fecal microbiota transplantation (FMT) from humans into mice could help identify transmissible factors that impact the brain's transcriptome. The results showed that a specific gut microbiome profile was linked to several memory domains and to the volume of hippocampus and prefrontal regions differentially in subjects with and without obesity. A plasma and fecal metabolomics signature associated with these traits was also identified. Importantly, the microbiota from obese subjects led to decreased short-term memory scores in recipient mice, which had shifts in aromatic amino acid (AAA) pathways and inflammatory genes in the prefrontal cortex (PFC) linked to clusters of bacterial species.

RESULTS AND DISCUSSION

Analysis of the Gut Metagenome Reveals Bacterial Gene Functions and Species Associated with Memory Scores

Memory function was evaluated in a cohort of 116 middle-aged subjects (n = 65 with obesity, n = 51 without obesity; Table 1). Impairments in learning, immediate recall, short delayed recall, and working memory were observed among subjects with obesity, based on the scores of California Verbal Learning Test

Figure 1. A Characteristic Microbiota Taxonomic and Functional Profile Is Associated with Memory Scores and Modulated by Obesity Status

(A and B) Boxplot for the total digit span (TDS) (A) and California Verbal Learning Short Delayed Free Recall (CVLT_SDFR) (B) in subjects with and without obesity. Differences between groups were analyzed by a Wilcoxon tests.

Immediate Recall (CVLT-IR), California Verbal Learning Test Short Delayed Free Recall (CVLT-SDFR), and Total Digit Span (TDS), respectively (Figures 1A, 1B, and S1A; Table 1).

A characteristic microbiome ecosystem was associated with cognitive scores using DESeq2 (Love et al., 2014) after adjusting for age, sex, BMI, years of education, and depression scores assessed using the Patient Health Questionnaire (PHQ)-9 (Figures 1C–1F, S1B, and S1C; Tables S1A–S1F). To take into account the compositional structure of the microbiome data and rule out possible spurious associations, we further analyzed the data using a compositional univariate approach (Table S2) with the ALDEx2 R package (Fernandes et al., 2014), as well as a multivariate machine learning feature selection strategy on the centered log-ratio transformed data (Table S3). Common species were positively associated with learning and verbal memory (CVLT-SDFR [Figure 1C; Tables S1A, S2A, and S3A]; CVLT-IR [Figure S1B; Table S1B]) and working memory (TDS [Figure 1D; Tables S1C, S2B, and S3B]), such as *Clostridium* sp. 27_14 or *Clostridium* sp. CAG:230, all of them belonging to Firmicutes phylum. On the contrary, negative associations between the gut microbiota and memory scores were identified within the phylum Bacteroides (*Bacteroides fragilis* CAG:558, *Bacteroides* sp. 43_46, *Bacteroides caccae* CAG:21, *Bacteroides* sp. HMSC067B03, and *Bacteroides* sp. AR20) and phylum Proteobacteria (*Citrobacter freundii*, *Enterobacter cloacae*, *Salmonella enterica*, and *Klebsiella aerogenes*).

Of note, while some species were positively and specifically associated with verbal learning, such as *Ruminococcus* sp. CAG:353, *Roseburia* sp. CAG:197, *Pararhodospirillum photometricum*, and *Veillonella magna* (Figures 1C and S1B; Tables S1A, S1B, S2A, and S3A), others were positively linked to working memory but not with learning or verbal memory (*Clostridium* sp. CAG:440, *Ruminococcus* sp. CAG:177, and *Firmicutes bacterium* CAG:103) (Figure 1D; Tables S1C, S2B, and S3B), suggesting divergent memory domains. Remarkably, several of the identified bacterial species were also longitudinally associated with the several memory domains measured one year later (Figure S2). The characteristics of these subjects are shown in Table 2.

Not only did the microbiota composition associate with memory, but also the metagenome functions were linked to this cognitive trait (Figures 1E, 1F, and S1C; Tables S1D–S1F, S2G, S2H, S3G, and S3H). Bacterial functions related to vitamin B metabolism, such as riboflavin (*ribBA*, *aphA*, *fre*, and *ubiB*), vitamin B6 (*pdxA*), folic acid (*pabB*, *queE*, *pabC*, *folM*, and *folX*), and vitamin B12 (*btuB*), were negatively associated with all memory domains (highlighted in black in Figures 1E, 1F, and S1 and in Tables S1D–S1F). Of note, all these vitamins are essential for one-carbon metabolism. There is convincing

data for the association between B vitamins and cognition (Mendonça et al., 2017; Obeid et al., 2007; Smith et al., 2010). In particular, it is well known that thiamine and folate impact memory (Matté et al., 2009; Witt and Goldman-Rakic, 1983). Bacterial functions involved in thiamine (vitamin B1) metabolism (*thiB*, *thiK*, and *ABC.VB1X.P*) were also associated with low memory scores. We hypothesized that these functions would result in preferential uptake or catabolism of thiamine by intestinal bacteria, resulting in decreased thiamine uptake by the host. Concordantly, significantly low plasma thiamine levels were found in subjects with lower memory scores (34.5 [27.2–45.3] versus 44.3 [32.3–64.6] ng/mL, p = 0.016). Other relevant metagenomic functions associated with several memory domains included those related to the AAA metabolism, one-carbon metabolism, and endocannabinoid signaling (highlighted in Figures 1E, 1F, and S1C and in Tables S1D–S1F) and are further discussed below.

When we evaluated the associations separately in subjects who were obese and non-obese (Figures 1G–1N and S1D–S1G; Tables S1G–S1R, S2C–S2F, and S3C–S3F), we found that several *Prevotella* sp. were positively associated with verbal memory among non-obese subjects (Figures 1G and S1D; Tables S1G, S1O, S2C, and S3C) while *Eubacterium* and *Clostridium* sp. showed similar associations within subjects with obesity (Figure 1I and S1E; Tables S1I, S1Q and S2D). Bacteria belonging to Proteobacteria phylum were similarly and negatively associated in subjects without and with obesity, but preferentially in the latter (Figures 1G and 1I; Tables S1I and S3D). Regarding working memory, we observed positive associations of *Selenomonadaceae*, *Lactococcus* sp., and *Colinsella* sp. in non-obese subjects (Figure 1K; Tables S1K, S2E, and S3E) and *Eubacterium sp.*, *Ruminococcus sp.*, *Clostridium sp.*, *and Faecalibacterium sp. CAG:74* in subjects with obesity (Figure 1M; Tables S1M, S2F, and S3F). The associations of bacterial functions related to thiamine were more marked among subjects with obesity (Figures 1J and 1N; Tables S1J, S1N, S2J, S2L, S3J, and S3L) who have been described to be particularly susceptible to thiamine deficits (Maguire et al., 2018).

In summary, several species of the phylum Firmicutes (belonging to *Clostridium*, *Ruminococcus*, and *Eubacterium* genera, and Selenomonadaceae family) were positively associated with memory scores. Species from the phyla Bacteroidetes and Proteobacteria mainly presented negative associations with memory scores.

To our knowledge, there are no previous descriptions of gut microbiota linked to the different memory domains in humans. Current results are in line with those identifying a higher prevalence of Bacteroidetes in patients with mild cognitive impairment (Saji et al., 2019). Species of the Enterobacteriaceae family such

---

(C and D) Volcano plots of differential bacterial abundance associated with the CVLT_SDFR (C) and the TDS (D), as calculated by DESeq2 from shotgun metagenomic sequencing in the IRONMET cohort, adjusting for age, BMI, sex, education years, and Patient Health Questionnaire (PHQ)-9 scores. Fold change (FC) associated with a unit change in the corresponding test and Benjamini-Hochberg-adjusted p values (pFDR) are plotted for each taxon. Significantly different taxa are colored according to phylum.

(E and F) Manhattan-like plot of significantly expressed KEGG bacterial genes associated with the CVLT_SDFR (pFDR < 0.002) (E) and TDS (pFDR < 0.04) (F), identified from DESeq2 analysis adjusted for age, BMI, sex, educations years, and PHQ-9. The -log₁₀(pFDR) values are multiplied by the FC sign to take into account the direction of the association. Bars are colored according to the pFDR. Those functions related to B vitamin metabolism, one-carbon metabolism, phenylalanine, tryptophan, and endocannabinoid metabolism are highlighted in black.

(G–N) Taxonomic and functional associations for the CVLT_SDFR and TDS tests in subjects with and without obesity. The complete list of significantly associated species and metagenomic functions can be found in Table S1.

Table 2. Clinical and Neuropsychological Data of the Human Follow-up Cohort

Total Population (Female n = 47, 68.1%)	Baseline (n = 69)	Follow-up (n = 69)	p
Age (years)	51.9 [44.3-59]	53 [45.4-60.2]	5.2×10^{-13}
BMI (kg/m^2)	28.2 [24.7-40.0]	28 [24.9-36.4]	0.192
Waist (cm)	103 [86.3-121.3]	97 [87-119]	0.044
Fat mass (%)	40.2 [32.7-49.7]	36.9 [31.8-46.9]	0.158
SBP (mmHg)	128 [118-141.8]	128 [118-138.3]	0.278
DBL (mmHg)	72.5 [67-82]	74 [67.8-80]	0.817
HDL-C (mg/dL)	58 [47-70.5]	57 [49-68.5]	0.601
Triglycerides (mg/dL)	86 [59-122]	88 [64-122]	0.796
FPG (mg/dL)	96 [89-102]	95 [90-102]	0.820
HbA1c (%)	5.5 [5.3-5.6]	5.5 [5.3-5.7]	0.317
hsCRP (mg/dL)	1.5 [0.6-5.1]	1.9 [0.7-3.3]	0.335
CVLT IR (score)	63 [56-70]	65 [60.5-72]	1.8×10^{-4}
CVLT SDFR (score)	14 [12-16]	15 [13.5-16]	0.005
Total Digit Span (score)	15 [12-17]	15 [12.5-17]	0.169
PHQ-9 (score)	5 [3-9]	4 [2-8]	0.209

Results are expressed as median and interquartile range [IQ]. To determine differences between study groups, we used paired Mann-Whitney U test. BMI, body mass index; SBP, systolic blood pressure; DBP, diastolic blood pressure; HDL-C, high density lipoprotein cholesterol; FPG, fasting plasma glucose; HbA1c, glycated hemoglobin; hsCRP, high-sensitive C-reactive protein; CVLT, California Verbal Learning Test; IR, Immediate Recall; SDFR, Short Delayed Free Recall; PHQ-9, Patient Health Questionnaire.

as *Citrobacter rodentium* (phylum Proteobacteria) were associated with impaired memory in acute stress (Gareau et al., 2011). *Ruminococcus gnavus* and different Bacteroidetes and Enterobacter species were increased in subjects with insulin resistance and obesity (Ley et al., 2006; Org et al., 2015) and associated with a worse cognitive profile (Tables S1A–S1C). Conversely, taxa of the phylum Firmicutes such as Clostridiales and *Roseburia* linked to higher memory score had a decreased relative abundance in subjects with type 2 diabetes (Tilg et al., 2020). In mice, the combined administration of *Lactobacillus rhamnosus* and *helveticus* led to increased non-spatial memory, improving c-Fos expression in the hippocampus (Gareau et al., 2011; Smith et al., 2014).

Brain Structure Differentially Associates with the Gut Microbiome and Bacterial Functions in Subjects Who Are Obese versus Non-obese

We evaluated the volume of different brain areas involved in verbal and working memory in 143 subjects using MRI (Table S4). Verbal and learning memory were associated with the volumes of the right and left hippocampus, and working memory with the right frontal inferior orbital (FIO) volume in all subjects after adjustment for age, BMI, sex, total intracranial volume (TIV), and PHQ-9 (from now on the term "adjusted" will refer to these adjustments) (Figure 2A). The hippocampal associa-

tions were also significant and positive within non-obese subjects, although no significant associations were found with the frontal areas (Figures 2B–2D). Conversely, working memory (TDS) was positively associated with the left FIO volume in all subjects (Figure 2A) and with other frontal areas within non-obese subjects (Figures 2B, 2E, and 2F). Notably, no significant associations among these memory domains and brain volumes were observed in individuals with obesity. The adjusted relationships between the baseline verbal and learning memory (free retrieval of words in CVLT tests) and the volumes of the right and left hippocampus as assessed one year later in 69 of the participants were also significant. These findings highlight different brain structures involved in verbal and working memory and are in line with previous reports linking verbal memory performance with prefrontal and temporal brain features, such as the hippocampus (Aslaksen et al., 2018; Colom et al., 2007; Gross et al., 2018; Yu et al., 2018). Interestingly, we found several *Roseburia sp*. positively associated with verbal memory that were directly associated with the adjusted volume of the left hippocampus, and also concordant negative associations among *Bacteroides sp*., verbal memory scores, and the adjusted volume of left hippocampus (Figure 2G; Table S5A). Other concordant associations are shown in bold in Figure 2G.

On the other hand, *Acetitomaculum ruminis* was concomitantly associated with working memory and the adjusted volume of the right FIO area (Figure 2H; Table S5D) while several *Bacteroides sp*. appeared negatively and concordantly associated with both verbal and working memory and the adjusted volume of both the left hippocampus and right FIO area (Figure 2H; Tables S5A and S5D). We also found several bacterial functions concordantly associated with memory scores and adjusted volumes (both positively and negatively), shown in bold in Figure 2I and Tables S5B and S5E. Of note, a function related to thiamine metabolism was associated with the adjusted right FIO volume.

Notably, the metagenomic functions found to be associated with the volume of the hippocampus were also associated with verbal memory, while those associated with the FIO volume were also concordantly linked to working memory. In addition, the bacterial taxonomy and metagenomic functions were associated with the volume of brain areas and memory domains not only at baseline but also at follow up (Figures S3A–S3D; Tables S5G–S5J).

When subjects with and without obesity were evaluated separately, several bacterial functions that were found to be significantly linked with verbal and working memory were also associated with the adjusted left hippocampus (Figure 2K) and right FIO volumes (Figure 2L), respectively, in subjects without obesity (shown in bold). Remarkably, no associations were found between metagenomic functions and these brain volumes in subjects with obesity, which is in line with the lack of significant associations between memory tests and selected brain volumes in subjects with obesity.

There is preliminary evidence that commensal bacteria are associated with morphological brain features in animal models (Lu et al., 2018; Luczynski et al., 2016). In addition, the gut microbiota composition at a single timepoint was associated with several brain features in humans (Labus et al., 2017; Tillisch
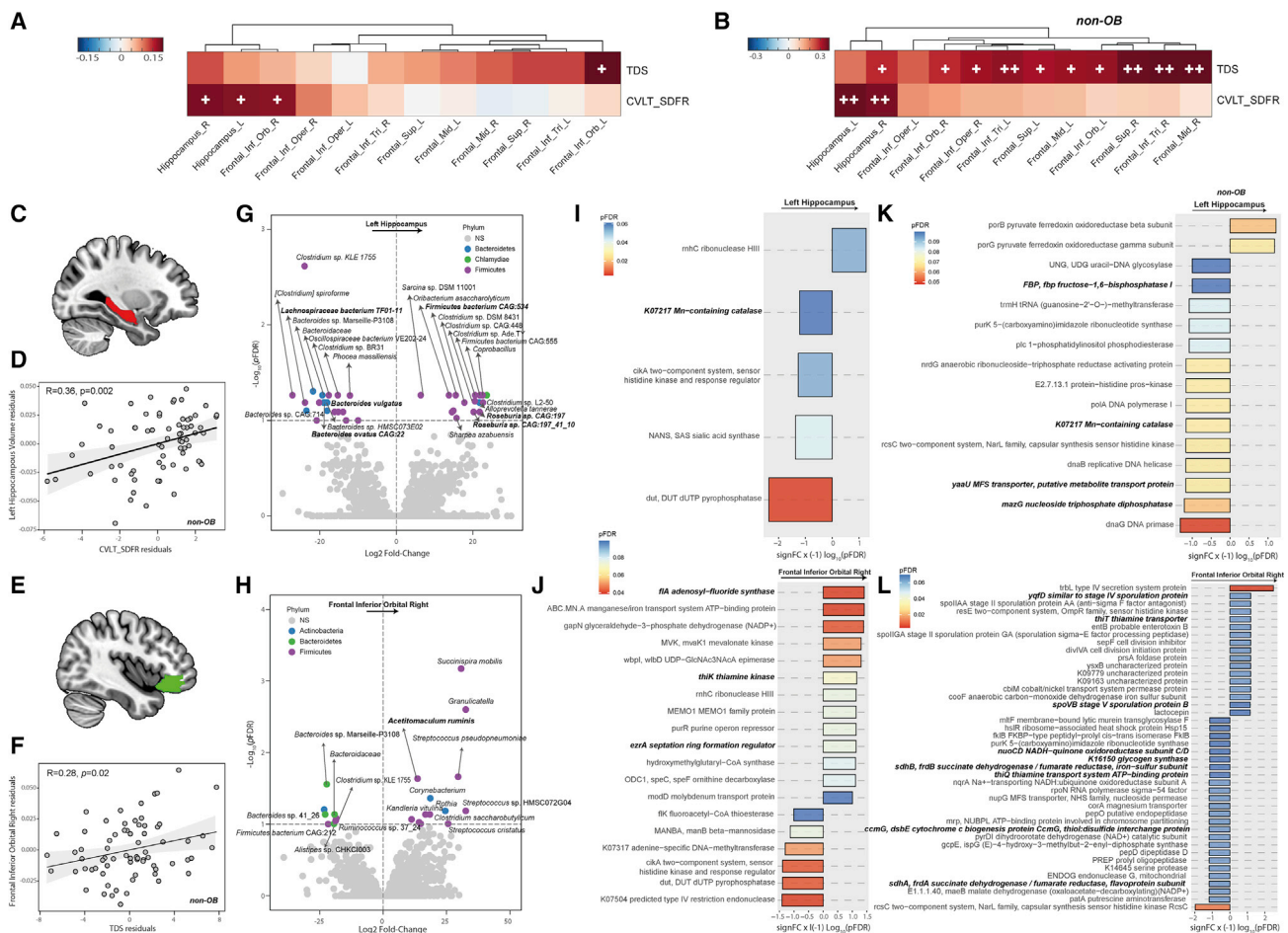
Figure 2. The Gut Microbiota Is Associated with Brain Structure

(A and B) Heatmap showing the partial correlations (adjusted by age, sex, BMI, education years, PHQ-9, and total intracranial volume [TIV]) between the TDS and CVLT_SDFR tests and selected brain volumes in all subjects with and without obesity (A) and subjects without obesity (B). Significant associations are shown with a cross: +, p < 0.05; ++ p < 0.01. No statistically significant associations were found in individuals with obesity and are not shown.

(C, D, E, and F) After controlling for the above covariates, the left hippocampus volume had a positive association with the CVLT_SDFR (C and D), whereas the right frontal inferior orbital volume was positively associated with the TDS (E and F). Both associations were more marked when only individuals without obesity were considered.

(G and H) Volcano plots of differential bacterial abundance associated with the left hippocampus volume (G) and right frontal inferior orbital volume (H), as calculated by DESeq2, controlling for covariates. Fold change (FC) associated with a unit change in the corresponding volumes and Benjamini-Hochberg-adjusted p values (*p*FDR) are plotted for each taxon. Significantly different taxa are colored according to phylum. Taxa that were also associated with the memory domains are highlighted in bold.

(I and J) Manhattan-like plot of significantly expressed KEGG bacterial genes associated with the left hippocampus volume (I) and right frontal inferior orbital volume (J), identified from covariate-adjusted DESeq2 analysis. The -log$_{10}$(*p*FDR) values are multiplied by the FC sign to take into account the direction of the association. Bars are colored according to the *p*FDR. Metagenomic functions that were also associated with the several cognitive domains are highlighted in bold.

(K and L) The results of the same functional analysis for the left hippocampus volume (K) and right frontal inferior orbital volume (L) in individuals without obesity. The complete list of associated functions can be found in Table S5. No significant functional associations were found in individuals with obesity for these brain volumes.

et al., 2017). For instance, in agreement with our findings, Tillisch and colleagues (2017) found greater Bacteroides abundance to be associated to larger gray matter volume in the hippocampus of healthy women. In patients with irritable bowel syndrome, the relative abundance of Firmicutes and Bacteroidetes showed a relationship with the gray matter volume of the opercula (orbital and triangularis sections) as well as with the temporal cortex (Labus et al., 2017).

Memory Scores Differentially Associate with Plasma/Fecal Metabolomics and Bacterial Functions in Subjects Who Are Obese versus Non-obese

We then performed metabolome-wide association studies (MWASs) using random forest-based machine learning variable selection techniques to identify plasma (Figures 3A–3H, S4A–S4H, and S5A–S5H) and fecal (Figures 3I–3P, S4I–S4P, and S5I–S4P) metabolites associated with the memory tests. Remarkably,
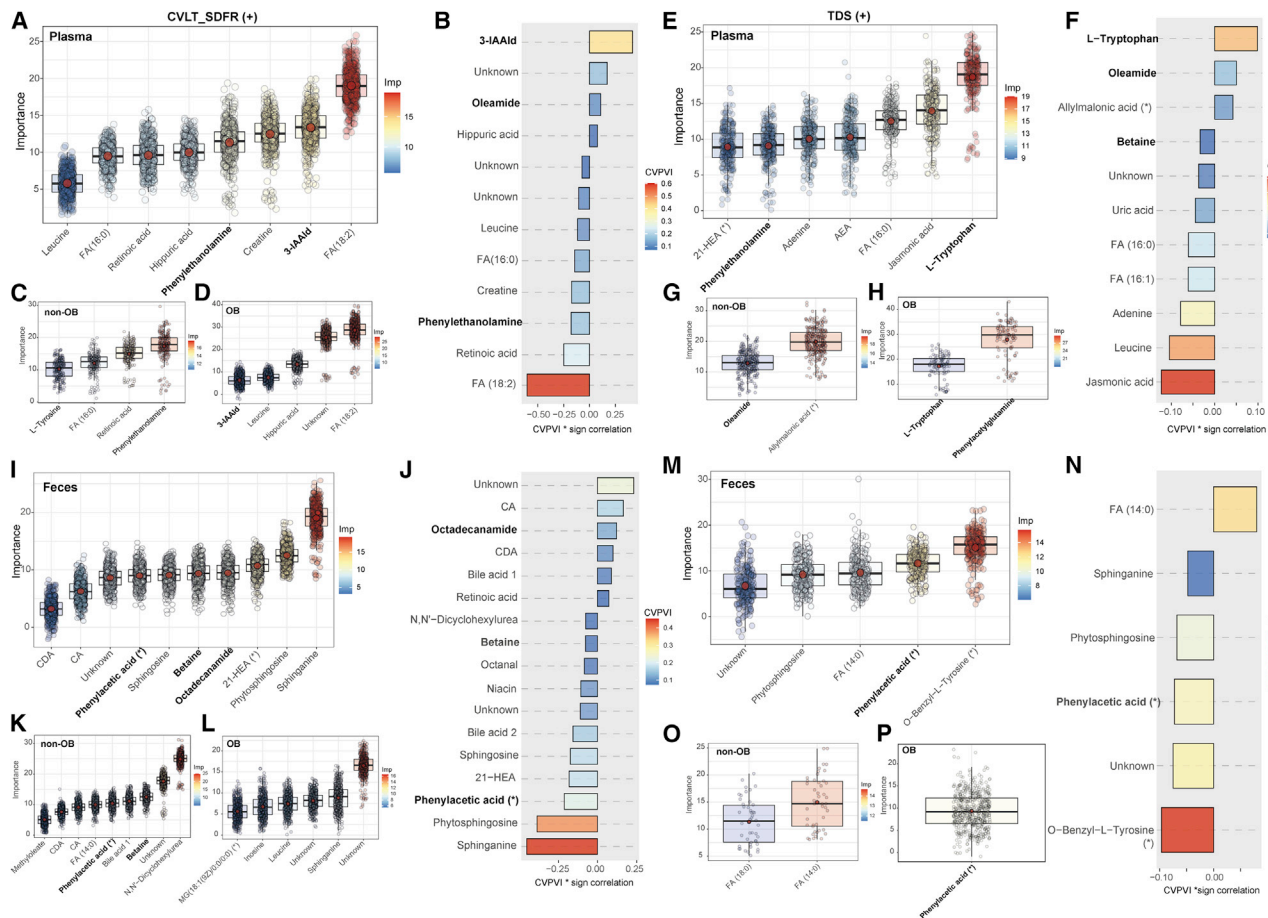
Figure 3. Plasma and Fecal Metabolomics in Electrospray Ionization (ESI) Positive Mode Linked to Memory Domains

(A, E, I, and M) Boxplots of the normalized permutation importance measure for the metabolites associated to the to the CVLT_SDFR in plasma (A), the TDS in plasma (E), the CVLT_SDFR in feces (I), and the TDS in feces (M), identified by machine learning thorough the random forest-based Boruta feature selection algorithm at each of the 500 iterations.

(B, F, J, and N) Cross-validated permutation variable importance (CVPVI) measure × sign of the correlation between each metabolite associated to the CVLT_SDFR test in plasma (B), the TDS in plasma (F), the CVLT_SDFR in feces (J), and the TDS in feces (N), identified by machine learning using the random forest-based Vita method.

(C, D, G, H, K, L, O, and P) Normalized permutation importance measure for Boruta selected metabolites associated to the CVLT_SDFR in plasma (C and D), the TDS in plasma (G and H), the CVLT_SDFR in plasma (K and L), and the TDS in feces (O and P), in individuals with and without obesity, respectively. All metabolites were identified based on exact mass, retention time and MS/MS spectrum, except those with (*) that were only identified based on exact mass and retention time. 3-IAAld, Indole-3-acetaldehyde; AEA, arachidonoylethanolamide; CA, cholic acid; CDA, chenodeoxycholic acid; FA, fatty acid.

the scores of all memory domains were associated with altered plasma levels of the AAAs tryptophan, tyrosine, and phenylalanine and their catabolites (Tryptophan catabolites: Indole-3-acetaldehyde [3-IAAld], Indole-3-propionic acid [3-IPA]; Tyrosine catabolites: 4-hydroxyphenyllactic acid [4-HPLA]; Phenylalanine catabolites: Phenylacetylglutamine and Phenylacetylglycine). These AAAs are the precursor amino acids of serotonin and dopamine, two neurotransmitters that play a key role in the central nervous system. Brain regions implicated in cognition, such as the hippocampus and the PFC, are vastly innervated by dopaminergic and serotonergic afferents, and alterations in both the serotonergic and dopaminergic neurotransmission are associated with impaired learning and memory (González-Burgos and Feria-Velasco, 2008; Švob Štrac et al., 2016). Both tryptophan and tyrosine positively associated with memory scores. This finding is in line

with past work where the oral administration of tryptophan led to improved memory acquisition, consolidation, and storage in rodents (Haider et al., 2007; Noristani et al., 2012).

Previous studies have shown that alterations of the microbiota due to antibiotic treatment resulted in decreased AAA concentrations and serotonin and dopamine levels in the porcine hypothalamus (Gao et al., 2018). The gut microbiota has also shown to directly metabolize tryptophan into several indole derivatives, which are potent ligands of the aryl hydrocarbon receptor (AhR). Deletion of the AhR alters adult hippocampal neurogenesis and contextual fear memory (de la Parra et al., 2018; Latchney et al., 2013). Consistently, we found several indole derivatives positively associated with memory scores. In addition, we also identified several bacterial functions involved in tryptophan and phenylalanine metabolism that negatively associated with the

different memory domains (Figures S1H and S1I; Tables S1D–S1F). In particular, functions related to tryptophan transporters such as tryptophan-specific transporter (*mtr*) and low-affinity tryptophan permease (*tnaB*) had negative associations with the CVLT-SDFR. Quinate dehydrogenase (*quiA*), involved in tryptophan, tyrosine, and phenylalanine metabolism, had the strongest negative association with CVLT. Notably, fecal quinic acid had, by far, the strongest negative association with the TDS scores, followed by tryptophan (Figures S4I and S4J). The negative association between fecal tryptophan and memory scores might be related either to its transformation into tryptophan metabolites (see below) or to its increased systemic absorption.

Interestingly, the memory-related alterations in tryptophan metabolism were only observed in individuals with obesity, aligning with associations of tryptophan-related metagenomic functions and memory domains in subjects with obesity, but not in subjects without obesity. Chronic low-grade inflammation is a hallmark of obesity, and the association between obesity and cognitive decline has recently been shown to be mediated by inflammation (Bourassa and Sbarra, 2017; Yang et al., 2020). Consistently, we found a strong positive association between BMI and hs-CRP (R = 0.71, p < 1 × 10^{-16}). Notably, more than 90% of tryptophan is metabolized through the kynurenine pathway, which is activated under inflammatory conditions (Wang et al., 2015). In line with this, plasma tryptophan levels had a negative correlation with the hs-CRP (R = −0.34, p < 3.3 × 10^{-4}). Importantly, microbial-derived products, including indoles, play a key role in the activation of indole-amine 2,3-dioxygenase (IDO), the rate-limiting enzyme in the kynurenine pathway (Gao et al., 2020). There is previous evidence that these metabolites have an effect on astrocytes to limit inflammation of the central nervous system in experimental models (Rothhammer et al., 2016). The current observations are the first in humans, to our knowledge, linking tryptophan and its metabolites to cognition.

Cholinergic systems have also been linked to cognitive processes such as attention and memory (Jeltsch-David et al., 2008). Hence, choline is the precursor of the neurotransmitter acetylcholine, but it can also be metabolized to betaine, a key methyl donor in the one-carbon metabolism and modulator of homocysteine status, whose elevated plasma levels have been implicated in learning and memory deficits (Mendonça et al., 2017). Thus, betaine supplementation has shown to prevent homocysteine-induced memory impairment via changes in the activity of MMP-9 in the frontal cortex (Kunisawa et al., 2015). In agreement, we found circulating betaine levels associated with memory scores. The changes in betaine levels are in line with the associations between cognitive domains and several metagenomic functions involved in choline and betaine transporters, such as choline/betaine transport protein (betT and betS), betaine/proline transport systems ATP-binding protein (proV), and betaine/proline transport systems substrate-binding protein (proX) (Tables S1D–S1F). Additionally, one of the functions most associated with short and immediate memory implicated the choline dehydrogenase (betA) gene (Tables S1D and S1E), responsible for the conversion of choline to betaine. Interestingly, we also found several alterations in metagenomic functions related to the metabolism of B vitamins involved in one-carbon metabolism, homocysteine levels, and cognition (Mendonça

et al., 2017; Obeid et al., 2007; Smith et al., 2010), mainly B2, B6, B9, and B12.

Other metabolites that had positive associations with the different memory domains were the endocannabinoids oleamide and arachidonoylethanolamide (AEA, anandamide). The endocannabinoids are lipid-derived mediators that play a key role in neurotransmission. Consequently, extensive evidence indicates a role of the endocannabinoid system in the modulation of cognition, particularly in learning and memory functioning (Maroso et al., 2016; Morena and Campolongo, 2014). Anandamide has been reported to reverse hippocampal damage and memory impairment in rodents and protect neurons from amyloid-β cytotoxic effects (van der Stelt et al., 2006). Similarly, oleamide administration significantly reversed memory and cognitive impairment in mice (Heo et al., 2003). Interestingly, we found that microbial N-acetyl Phosphatidylethanolamine Phospholipase D (NAPEPLD) (Figures 1F and 4H; Tables S1D and S1F), which is necessary for the biosynthesis of fatty acid ethanolamides, including the endocannabinoids (Basavarajappa, 2007), had one of the strongest associations with the cognitive domains of both humans and mice.

Effects of Microbiota Transplantation from Humans to Mice

We then tested the possible effects of the microbiota on memory scores in mice. The mouse behavioral models used in this study evaluated two different memory tasks. The cue-induced fear conditioning is a well-recognized model of emotional memories (Sun et al., 2020), whereas the novel object recognition paradigm is a widely used model of memories with a different neurobiological substrate (Puighermanal et al., 2009). Specifically, cue-induced fear conditioning evaluates emotional memory by assessing mice ability to associate neutral cues with an aversive experience, in which behavioral responses are mainly mediated by the amygdala (Barsy et al., 2020). The subsequent presentation of the cue retrieves the memory trace and initiates a conditioned response; freezing, driven by the central amygdala (Sun et al., 2020). In contrast, the hippocampus plays a crucial role in the memory responses evaluated in the novel object recognition paradigm. The long-term memory traces evaluated in this paradigm are related to spatial memories not related to emotional aspects (Puighermanal et al., 2009).

The novel object recognition cognitive task was performed using a V maze, since the accuracy and reliability of the behavioral response is improved when compared to the use of an open field for this task. In this task, the exploration of the mouse is directed to the two different objects located in the extremes of the V maze (Puighermanal et al., 2009; Busquets-Garcia et al., 2013).

Microbiota from 22 human subjects (11 with low and 11 with high memory scores matched for age, sex, BMI, and PHQ-9 scores) (Table S6) was orally delivered to individual mice in a blinded fashion (the investigator who performed the experiment was blinded regarding the origin of feces). The effects on memory were compared with those of saline in 11 control mice. All mice were pretreated with antibiotics for 14 days (Figure 4A). Mice receiving FMT had higher scores in the Novel Object Recognition test at 24 h (NOR24 h) and lower Freezing Total scores than control mice (Figures 4B and S6A). Interestingly, microbiota from non-obese donors led to significantly increased NORII24 h scores compared with both obese donors (p = 0.026)
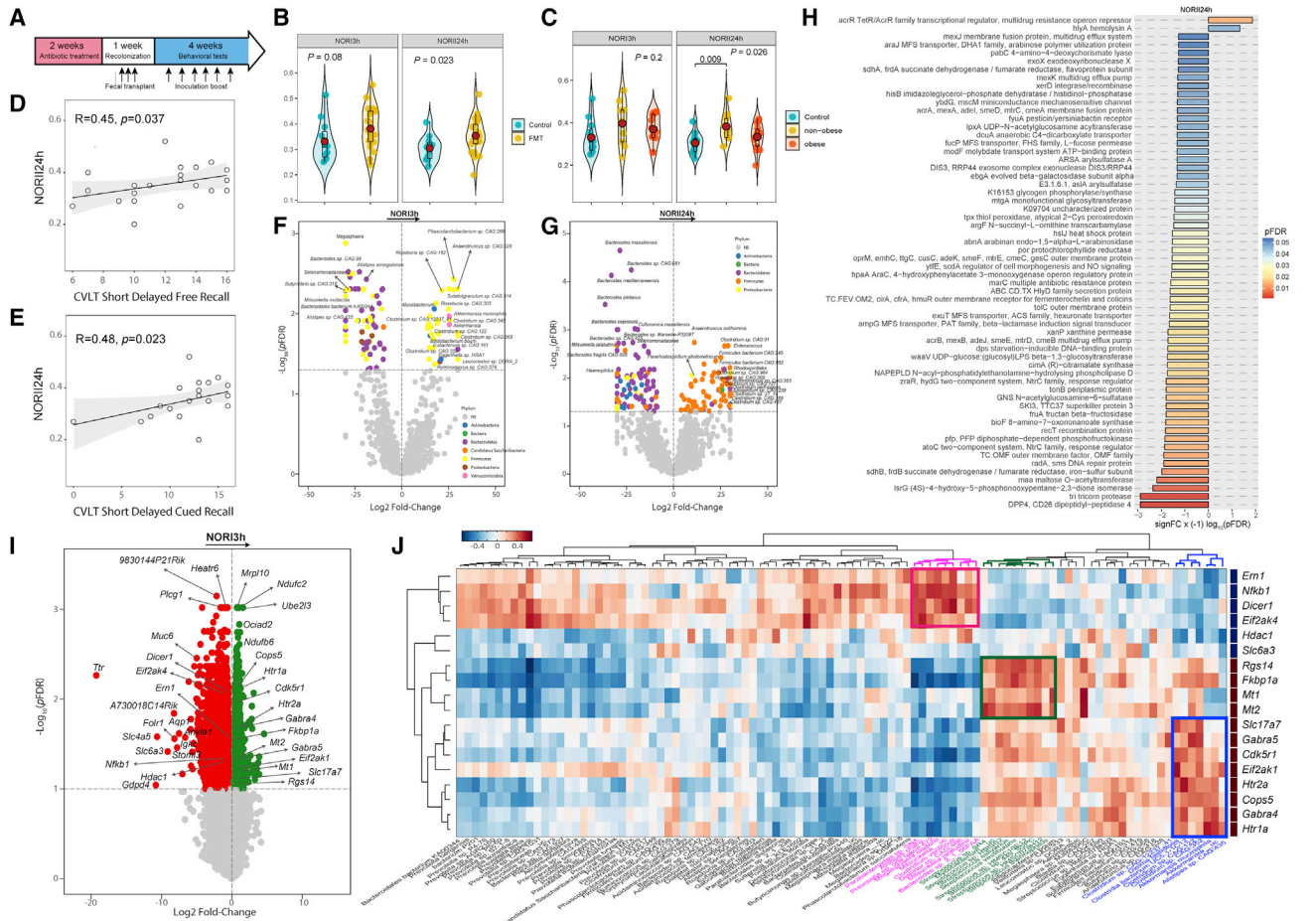
Figure 4. Human Donor's and Recipient's Mice Memory Became Aligned through the Microbiota

(A) Experimental design for the fecal microbiota transplantation (FMT) study. The microbiota from low-memory (n = 11) and high-memory (n = 11) human donors were delivered to recipient mice pre-treated with antibiotics for 14 days. n = 11 control mice were treated with saline. Cognitive tests were performed after 4 weeks.

(B and C) Violin plots for the Novel Object Recognition tests comparing the control group and the FMT group (t test) (B), and comparing the control group to the groups receiving microbiota from human donors with and without obesity (one-way ANOVA) (C).

(D and E) Spearman correlation between the California Verbal Learning tests (CVLTs) in humans and the NOR24 h in mice.

(F and G) Volcano plots of differential human donor bacterial abundance associated with the recipient's mice NOR3 h (F) and the NOR24 h (G), from DESeq2 analysis. Fold change (FC) associated with a unit change in the corresponding memory test and Benjamini-Hochberg-adjusted p values (*p*FDR) are plotted for each taxon. Significantly different taxa are colored according to phylum.

(H) Manhattan-like plot showing only the significantly expressed KEGG bacterial genes associated with the mice NOR 24 h test (*p*FDR < 0.05) that were also associated to the total digit span score in humans. The -log₁₀(*p*FDR) values are multiplied by the FC sign to take into account the direction of the association. Bars are colored according to the *p*FDR. A complete list of significantly associated bacterial genes can be found in Table S5C.

(I) Volcano plot of differential prefrontal cortex (PFC) genes associated with the NOR3 h. FC associated with a unit change in the NOR3 h test and Benjamini-Hochberg-adjusted p values (*p*FDR) are plotted for each gene. Those genes with the highest FC and the lowest *p*FDR values are highlighted. Genes with a possible role in memory based on the literature are also highlighted.

(J) Correlation heatmap among mice bacterial species and selected PFC genes associated with NOR3 h. Clustering was performed using Euclidean distances and Ward linkage. Three bacterial clusters with strong correlations were identified and highlighted. These involve bacterial species positively linked to both the NOR3 h and PFC genes positively associated with the NOR3 h, and bacterial species negatively associated to the NOR3 h and at the same negatively associated to PFC genes positively associated with the NOR3 h and positively associated to genes negatively associated with the NOR3 h.

and control mice (p = 0.009) (Figure 4C). Of note, both donor's CVLT-SDFR and CVLT-Short Delayed Cued Recall scores were significantly correlated with NOR24 h scores in recipient mice (Figures 4D and 4E). Bacterial species from the donor's microbiota, including *Akkermansia sp*. and *Subdoligranulum sp*. (NOR3 h) (Figure 4F; Table S7A), and *Clostridium*, *Ruminococcus*, and *Roseburia sp*. (NOR24 h) (Figure 4G; Table S7B),

were associated with increased memory scores of recipient mice, while several *Bacteroides sp*. were negatively associated with this score. Accordingly, the same *Bacteroides* sp. were positively associated with the Freezing Total scores (Figure S6C). Notably, several donors' metagenomic functions, including the *NAPEPLD,* associated with the TDS memory domains of the donor and with the NOR24 h scores of recipient mice (Figure 4H).

Further, in line with the human results, other associated functions included those related to vitamin B6 (*pdxJ* and *pdxB*), B12 (*btuB*), and tryptophan metabolism (*trpA* and *trpB*) (Table S7C).

Finally, an RNA sequencing of the PFC of the mice highlighted several significant genes associated with the NOR3 h score (Figure 4I; Table S7D). In the test phase, different memory scores were recorded: mice were studied 3 h later for short-term memory (NOR3 h) and 24 h later for long-term memory (NOR24h). Notably, the gene with the highest negative fold change was transthyretin (*ttr*), which has been shown to have altered hippocampal expression associated with memory deficits in aged animals (Brouillette and Quirion, 2008). The gene with the second strongest fold change was *slc6a3,* which encodes a dopamine transporter. In addition, there was a direct association between NORI3 h and the 5HT receptor genes *htr1a* and *htr2a*, as well as the folate receptor gene *folr1*, further emphasizing the connection between AAAs, folate metabolism, and memory. The nuclear factor gene *nfkb1*, known to be crucial in the inflammatory cascade and in memory consolidation (Snow et al., 2014), was also directly associated to short-term memory; whereas *dicer1* was negatively associated with this memory trait. Relatedly, the knockout of *dicer1* has been previously reported to enhance memory (Konopka et al., 2010). Finally, *acss2* and *hdac1* were directly associated to short-term memory, confirming recent observations of brain histone acetylation relationships with associative learning (Mews et al., 2017). Interestingly, the expression of the memory genes associated to the NORI3 h was simultaneously associated with different bacterial clusters and in the same direction (Figure 4J).

Altogether, the current findings point to the existence of an ecosystem of bacteria that are simultaneously linked to verbal and working memory, the volume of brain areas involved in these traits, plasma/fecal tryptophan, microbiota-driven tryptophan metabolites, and 5HT receptor expression in the PFC. Several of the species identified here have been previously linked with positive (Roseburia, Subdoligranulum, and Faecalibacterium) and negative (Fusobacterium and Bacteroides) healthy eating scores (Liu et al., 2019) in the same direction as the increased and decreased memory scores described here. These findings suggest a bidirectional host/microbe ecosystem that impacts brain physiology. In this sense, the gut microbiota phenocopied memory traits from humans to mice.

Limitations of Study

The current study presents some limitations. Although the sample size of the different cohorts seems appropriate, population-based studies including subjects with different classes of obesity and ethnic groups would be more representative of this condition. In addition, although our conclusions are based on the findings of cross-sectional and one-year longitudinal studies, longer term follow-up would be necessary to better understand the strength of our conclusions. Finally, regarding the mouse models, despite being widely used and validated to infer cognitive function in real settings, they cannot be exactly comparable with cognitive evaluation and brain morphology in humans.

STAR★METHODS

Detailed methods are provided in the online version of this paper and include the following:

- KEY RESOURCES TABLE
- RESOURCE AVAILABILITY
  - Lead Contact
  - Materials Availability
  - Data and Code Availability
- EXPERIMENTAL MODEL AND SUBJECT DETAILS
  - Clinical Study
  - Longitudinal Cohort
  - Animal Study
- METHOD DETAILS
  - Clinical and Laboratory Parameters
  - Magnetic Resonance Imaging (MRI)
  - Neuropsychological Assessment in Humans
  - Extraction of Fecal Genomic DNA and Whole-Genome Shotgun Sequencing
  - Metabolomics Analyses
  - Behavioral Testing in Mice
  - Study of Gene Expression in Prefrontal Cortex
- QUANTIFICATION AND STATISTICAL ANALYSIS

reviewed the manuscript. M.J., J.S., R.P., and M.P.-O. performed the metabolomics analyses and contributed in writing the corresponding parts of the paper associated with the metabolomics data. J.M.F.-R. carried out the conception and coordination of the study, performed the statistical analysis, and wrote the manuscript. All authors participated in final approval of the version to be published. J.M.F.-R. is the guarantor of this work and, as such, had full access to all the data in the study and takes responsibility for the integrity of the data.

REFERENCES

Arnoriaga-Rodríguez, M., and Fernández-Real, J.M. (2019). Microbiota impacts on chronic inflammation and metabolic syndrome - related cognitive dysfunction. Rev. Endocr. Metab. Disord. 20, 473–480.

Aslaksen, P.M., Bystad, M.K., Ørbo, M.C., and Vangberg, T.R. (2018). The relation of hippocampal subfield volumes to verbal episodic memory measured by the California Verbal Learning Test II in healthy adults. Behav. Brain Res. 351, 131–137.

Barsy, B., Kocsis, K., Magyar, A., Babiczky, Á., Szabó, M., Veres, J.M., Hillier, D., Ulbert, I., Yizhar, O., and Mátyás, F. (2020). Associative and plastic thalamic signaling to the lateral amygdala controls fear behavior. Nat. Neurosci. 23, 625–637.

Basavarajappa, B.S. (2007). Critical enzymes involved in endocannabinoid metabolism. Protein Pept. Lett. 14, 237–246.

Blasco, G., Moreno-Navarrete, J.M., Rivero, M., Pérez-Brocal, V., Garre-Olmo, J., Puig, J., Daunis-I-Estadella, P., Biarnés, C., Gich, J., Fernández-Aranda, F., et al. (2017). The Gut Metagenome Changes in Parallel to Waist Circumference, Brain Iron Deposition, and Cognitive Function. J. Clin. Endocrinol. Metab. 102, 2962–2973.

Bourassa, K., and Sbarra, D.A. (2017). Body mass and cognitive decline are indirectly associated via inflammation among aging adults. Brain Behav. Immun. 60, 63–70.

Brouillette, J., and Quirion, R. (2008). Transthyretin: a key gene involved in the maintenance of memory capacities during aging. Neurobiol. Aging 29, 1721–1732.

Brunkwall, L., and Orho-Melander, M. (2017). The gut microbiome as a target for prevention and treatment of hyperglycaemia in type 2 diabetes: from current human evidence to future possibilities. Diabetologia 60, 943–951.

Burokas, A., Martín-García, E., Gutiérrez-Cuesta, J., Rojas, S., Herance, J.R., Gispert, J.D., Serra, M.-Á., and Maldonado, R. (2014). Relationships between serotonergic and cannabinoid system in depressive-like behavior: a PET study with [11C]-DASB. J. Neurochem. 130, 126–135.

Burokas, A., Arboleya, S., Moloney, R.D., Peterson, V.L., Murphy, K., Clarke, G., Stanton, C., Dinan, T.G., and Cryan, J.F. (2017). Targeting the Microbiota-Gut-Brain Axis: Prebiotics Have Anxiolytic and Antidepressant-like Effects and Reverse the Impact of Chronic Stress in Mice. Biol. Psychiatry 82, 472–487.

Busquets-Garcia, A., Gomis-González, M., Guegan, T., Agustín-Pavón, C., Pastor, A., Mato, S., Pérez-Samartín, A., Matute, C., De la Torre, R., Dierssen, M., et al. (2013). Targeting the endocannabinoid system in the treatment of fragile X syndrome. Nat. Med. 19, 603–607.

Chu, C., Murdock, M.H., Jing, D., Won, T.H., Chung, H., Kressel, A.M., Tsaava, T., Addorisio, M.E., Putzel, G.G., Zhou, L., et al. (2019). The microbiota regulate neuronal function and fear extinction learning. Nature 574, 543–548.

Colom, R., Jung, R.E., and Haier, R.J. (2007). General intelligence and memory span: evidence for a common neuroanatomic framework. Cogn. Neuropsychol. 24, 867–878.

Cournot, M., Marquié, J.C., Ansiau, D., Martinaud, C., Fonds, H., Ferrières, J., and Ruidavets, J.B. (2006). Relation between body mass index and cognitive function in healthy middle-aged men and women. Neurology 67, 1208–1214.

de la Parra, J., Cuartero, M.I., Pérez-Ruiz, A., García-Culebras, A., Martín, R., Sánchez-Prieto, J., García-Segura, J.M., Lizasoain, I., and Moro, M.A. (2018). AhR deletion promotes aberrant morphogenesis and synaptic activity of adult-generated granule neurons and impairs hippocampus-dependent memory. eNeuro 5, 1–20.

Degenhardt, F., Seifert, S., and Szymczak, S. (2019). Evaluation of variable selection methods for random forests and omics data sets. Brief. Bioinform. 20, 492–503.

Delis, D.C., Kramer, J.H., Kaplan, E., and Ober, B.A. (2000). Manual for the California Verbal Learning Test, (CVLT-II) (The Psychological Corporation).

Dobin, A., Davis, C.A., Schlesinger, F., Drenkow, J., Zaleski, C., Jha, S., Batut, P., Chaisson, M., and Gingeras, T.R. (2013). STAR: ultrafast universal RNA-seq aligner. Bioinformatics 29, 15–21.

Durbin, R., Eddy, S.R., Krogh, A., and Mitchison, G. (1998). Biological Sequence Analysis: Probabilistic Models of Proteins and Nucleic Acids (Cambridge University Press).

Fernandes, A.D., Reid, J.N.S., Macklaim, J.M., McMurrough, T.A., Edgell, D.R., and Gloor, G.B. (2014). Unifying the analysis of high-throughput sequencing datasets: characterizing RNA-seq, 16S rRNA gene sequencing and selective growth experiments by compositional data analysis. Microbiome 2, 15.

Fernandez-Real, J.M., Serino, M., Blasco, G., Puig, J., Daunis-i-Estadella, J., Ricart, W., Burcelin, R., Fernández-Aranda, F., and Portero-Otin, M. (2015). Gut microbiota interacts with brain microstructure and function. J. Clin. Endocrinol. Metab. 100, 4505–4513.

Gao, K., Pi, Y., Mu, C.L., Peng, Y., Huang, Z., and Zhu, W.Y. (2018). Antibiotics-induced modulation of large intestinal microbiota altered aromatic amino acid profile and expression of neurotransmitters in the hypothalamus of piglets. J. Neurochem. 146, 219–234.

Gao, K., Mu, C.L., Farzi, A., and Zhu, W.Y. (2020). Tryptophan Metabolism: A Link Between the Gut Microbiota and Brain. Adv. Nutr. 11, 709–723.

Gareau, M.G., Wine, E., Rodrigues, D.M., Cho, J.H., Whary, M.T., Philpott, D.J., Macqueen, G., and Sherman, P.M. (2011). Bacterial infection causes stress-induced memory dysfunction in mice. Gut 60, 307–317.

González-Burgos, I., and Feria-Velasco, A. (2008). Serotonin/dopamine interaction in memory formation. Prog. Brain Res. 172, 603–623.

Gross, L.A., Moore, E.M., Wozniak, J.R., Coles, C.D., Kable, J.A., Sowell, E.R., Jones, K.L., Riley, E.P., and Mattson, S.N.; CIFASD (2018). Neural correlates of verbal memory in youth with heavy prenatal alcohol exposure. Brain Imaging Behav. 12, 806–822.

Gunstad, J., Paul, R.H., Cohen, R.A., Tate, D.F., and Gordon, E. (2006). Obesity is associated with memory deficits in young and middle-aged adults. Eat. Weight Disord. 11, e15–e19.

Gunstad, J., Sanborn, V., and Hawkins, M. (2020). Cognitive dysfunction is a risk factor for overeating and obesity. Am. Psychol. 75, 219–234.

Haider, S., Khaliq, S., and Haleem, D.J. (2007). Enhanced serotonergic neurotransmission in the hippocampus following tryptophan administration improves learning acquisition and memory consolidation in rats. Pharmacol. Rep. 59, 53–57.

Heo, H.J., Park, Y.J., Suh, Y.M., Choi, S.J., Kim, M.J., Cho, H.Y., Chang, Y.J., Hong, B., Kim, H.K., Kim, E., et al. (2003). Effects of oleamide on choline acetyltransferase and cognitive activities. Biosci. Biotechnol. Biochem. 67, 1284–1291.

Hyatt, D., Chen, G.L., Locascio, P.F., Land, M.L., Larimer, F.W., and Hauser, L.J. (2010). Prodigal: prokaryotic gene recognition and translation initiation site identification. BMC Bioinformatics 11, 119.

Janitza, S., Celik, E., and Boulesteix, A.-L. (2018). A computationally fast variable importance test for random forests for high-dimensional data. Adv. Data Anal. Classif. 12, 885–915.

Jeltsch-David, H., Koenig, J., and Cassel, J.C. (2008). Modulation of cholinergic functions by serotonin and possible implications in memory: general

data and focus on 5-HT(1A) receptors of the medial septum. Behav. Brain Res. *195*, 86–97.

Kanehisa, M., and Goto, S. (2000). KEGG: Kyoto Encyclopedia of Genes and Genomes. Nucleic Acids Res. *28*, 27–30.

Kelly, J.R., Borre, Y., O' Brien, C., Patterson, E., El Aidy, S., Deane, J., Kennedy, P.J., Beers, S., Scott, K., Moloney, G., et al. (2016). Transferring the blues: Depression-associated gut microbiota induces neurobehavioural changes in the rat. J. Psychiatr. Res. *82*, 109–118.

Kivipelto, M., Mangialasche, F., and Ngandu, T. (2018). Lifestyle interventions to prevent cognitive impairment, dementia and Alzheimer disease. Nat. Rev. Neurol. *14*, 653–666.

Konopka, W., Kiryk, A., Novak, M., Herwerth, M., Parkitna, J.R., Wawrzyniak, M., Kowarsch, A., Michaluk, P., Dzwonek, J., Arnsperger, T., et al. (2010). MicroRNA loss enhances learning and memory in mice. J. Neurosci. *30*, 14835–14842.

Kunisawa, K., Nakashima, N., Nagao, M., Nomura, T., Kinoshita, S., and Hiramatsu, M. (2015). Betaine prevents homocysteine-induced memory impairment via matrix metalloproteinase-9 in the frontal cortex. Behav. Brain Res. *292*, 36–43.

Kursa, M.B., and Rudnicki, W.R. (2010). Feature selection with the boruta package. J. Stat. Softw. *36*, 1–13.

Labus, J.S., Hollister, E.B., Jacobs, J., Kirbach, K., Oezguen, N., Gupta, A., Acosta, J., Luna, R.A., Aagaard, K., Versalovic, J., et al. (2017). Differences in gut microbial composition correlate with regional brain volumes in irritable bowel syndrome. Microbiome *5*, 49.

Langmead, B., and Salzberg, S.L. (2012). Fast gapped-read alignment with Bowtie 2. Nat. Methods *9*, 357–359.

Larson, E.B., Yaffe, K., and Langa, K.M. (2013). New insights into the dementia epidemic. N. Engl. J. Med. *369*, 2275–2277.

Latchney, S.E., Hein, A.M., O'Banion, M.K., DiCicco-Bloom, E., and Opanashuk, L.A. (2013). Deletion or activation of the aryl hydrocarbon receptor alters adult hippocampal neurogenesis and contextual fear memory. J. Neurochem. *125*, 430–445.

Ley, R.E., Turnbaugh, P.J., Klein, S., and Gordon, J.I. (2006). Microbial ecology: human gut microbes associated with obesity. Nature *444*, 1022–1023.

Li, D., Liu, C.M., Luo, R., Sadakane, K., and Lam, T.W. (2015). MEGAHIT: an ultra-fast single-node solution for large and complex metagenomics assembly via succinct de Bruijn graph. Bioinformatics *31*, 1674–1676.

Liao, Y., Smyth, G.K., and Shi, W. (2014). featureCounts: an efficient general purpose program for assigning sequence reads to genomic features. Bioinformatics *30*, 923–930.

Liu, Y., Ajami, N.J., El-Serag, H.B., Hair, C., Graham, D.Y., White, D.L., Chen, L., Wang, Z., Plew, S., Kramer, J., et al. (2019). Dietary quality and the colonic mucosa-associated gut microbiome in humans. Am. J. Clin. Nutr. *110*, 701–712.

Livingston, G., Sommerlad, A., Orgeta, V., Costafreda, S.G., Huntley, J., Ames, D., Ballard, C., Banerjee, S., Burns, A., Cohen-Mansfield, J., et al. (2017). Dementia prevention, intervention, and care. Lancet *390*, 2673–2734.

Love, M.I., Huber, W., and Anders, S. (2014). Moderated estimation of fold change and dispersion for RNA-seq data with DESeq2. Genome Biol. *15*, 550.

Lu, J., Synowiec, S., Lu, L., Yu, Y., Bretherick, T., Takada, S., Yarnykh, V., Caplan, J., Caplan, M., Claud, E.C., and Drobyshevsky, A. (2018). Microbiota influence the development of the brain and behaviors in C57BL/6J mice. PLoS ONE *13*, e0201829.

Luczynski, P., Whelan, S.O., O'Sullivan, C., Clarke, G., Shanahan, F., Dinan, T.G., and Cryan, J.F. (2016). Adult microbiota-deficient mice have distinct dendritic morphological changes: differential effects in the amygdala and hippocampus. Eur. J. Neurosci. *44*, 2654–2666.

Magoč, T., and Salzberg, S.L. (2011). FLASH: fast length adjustment of short reads to improve genome assemblies. Bioinformatics *27*, 2957–2963.

Maguire, D., Talwar, D., Shiels, P.G., and McMillan, D. (2018). The role of thiamine dependent enzymes in obesity and obesity related chronic disease states: A systematic review. Clin. Nutr. ESPEN *25*, 8–17.

Mao, J.-H., Kim, Y.-M., Zhou, Y.-X., Hu, D., Zhong, C., Chang, H., Brislawn, C.J., Fansler, S., Langley, S., Wang, Y., et al. (2020). Genetic and metabolic links between the murine microbiome and memory. Microbiome *8*, 53.

Maroso, M., Szabo, G.G., Kim, H.K., Alexander, A., Bui, A.D., Lee, S.H., Lutz, B., and Soltesz, I. (2016). Cannabinoid Control of Learning and Memory through HCN Channels. Neuron *89*, 1059–1073.

Maruvada, P., Leone, V., Kaplan, L.M., and Chang, E.B. (2017). The Human Microbiome and Obesity: Moving beyond Associations. Cell Host Microbe *22*, 589–599.

Matté, C., Pereira, L.O., Dos Santos, T.M., Mackedanz, V., Cunha, A.A., Netto, C.A., and Wyse, A.T.S. (2009). Acute homocysteine administration impairs memory consolidation on inhibitory avoidance task and decreases hippocampal brain-derived neurotrophic factor immunocontent: prevention by folic acid treatment. Neuroscience *163*, 1039–1045.

Mendonça, N., Granic, A., Mathers, J.C., Martin-Ruiz, C., Wesnes, K.A., Seal, C.J., Jagger, C., and Hill, T.R. (2017). One-Carbon Metabolism Biomarkers and Cognitive Decline in the Very Old: The Newcastle 85+ Study. J. Am. Med. Dir. Assoc. *18*, 806.e19–806.e27.

Menzel, P., Ng, K.L., and Krogh, A. (2016). Fast and sensitive taxonomic classification for metagenomics with Kaiju. Nat. Commun. *7*, 11257.

Mews, P., Donahue, G., Drake, A.M., Luczak, V., Abel, T., and Berger, S.L. (2017). Acetyl-CoA synthetase regulates histone acetylation and hippocampal memory. Nature *546*, 381–386.

Morena, M., and Campolongo, P. (2014). The endocannabinoid system: an emotional buffer in the modulation of memory function. Neurobiol. Learn. Mem. *112*, 30–43.

Noristani, H.N., Verkhratsky, A., and Rodríguez, J.J. (2012). High tryptophan diet reduces CA1 intraneuronal β-amyloid in the triple transgenic mouse model of Alzheimer's disease. Aging Cell *11*, 810–822.

Obeid, R., McCaddon, A., and Herrmann, W. (2007). The role of hyperhomocysteinemia and B-vitamin deficiency in neurological and psychiatric diseases. Clin. Chem. Lab. Med. *45*, 1590–1606.

Ohland, C.L., Kish, L., Bell, H., Thiesen, A., Hotte, N., Pankiv, E., and Madsen, K.L. (2013). Effects of Lactobacillus helveticus on murine behavior are dependent on diet and genotype and correlate with alterations in the gut microbiome. Psychoneuroendocrinology *38*, 1738–1747.

Org, E., Parks, B.W., Joo, J.W.J., Emert, B., Schwartzman, W., Kang, E.Y., Mehrabian, M., Pan, C., Knight, R., Gunsalus, R., et al. (2015). Genetic and environmental control of host-gut microbiota interactions. Genome Res. *25*, 1558–1569.

Palomo-Buitrago, M.E., Sabater-Masdeu, M., Moreno-Navarrete, J.M., Caballano-Infantes, E., Arnoriaga-Rodríguez, M., Coll, C., Ramió, L., Palomino-Schätzlein, M., Gutiérrez-Carcedo, P., Pérez-Brocal, V., et al. (2019). Glutamate interactions with obesity, insulin resistance, cognition and gut microbiota composition. Acta Diabetol. *56*, 569–579.

Paolo, A.M., Tröster, A.I., and Ryan, J.J. (1997). Test-retest stability of the California verbal learning test in older persons. Neuropsychology *11*, 613–616.

Paxinos, G., and Franklin, K.B.J. (1997). The mouse brain in stereotaxic coordinates (Academic Press).

Petersen, R.C., Smith, G.E., Waring, S.C., Ivnik, R.J., Tangalos, E.G., and Kokmen, E. (1999). Mild cognitive impairment: clinical characterization and outcome. Arch. Neurol. *56*, 303–308.

Puighermanal, E., Marsicano, G., Busquets-Garcia, A., Lutz, B., Maldonado, R., and Ozaita, A. (2009). Cannabinoid modulation of hippocampal long-term memory is mediated by mTOR signaling. Nat. Neurosci. *12*, 1152–1158.

R Development Core Team (2013). R: A Language and Environment for Statistical Computing.

Robinson, M.D., and Oshlack, A. (2010). A scaling normalization method for differential expression analysis of RNA-seq data. Genome Biol. *11*, R25.

Robinson, M.D., McCarthy, D.J., and Smyth, G.K. (2010). edgeR: a Bioconductor package for differential expression analysis of digital gene expression data. Bioinformatics *26*, 139–140.

Rogers, G.B., Keating, D.J., Young, R.L., Wong, M.L., Licinio, J., and Wesselingh, S. (2016). From gut dysbiosis to altered brain function and mental illness: mechanisms and pathways. Mol. Psychiatry 21, 738–748.

Rothhammer, V., Mascanfroni, I.D., Bunse, L., Takenaka, M.C., Kenison, J.E., Mayo, L., Chao, C.C., Patel, B., Yan, R., Blain, M., et al. (2016). Type I interferons and microbial metabolites of tryptophan modulate astrocyte activity and central nervous system inflammation via the aryl hydrocarbon receptor. Nat. Med. 22, 586–597.

Saji, N., Murotani, K., Hisada, T., Tsuduki, T., Sugimoto, T., Kimura, A., Niida, S., Toba, K., and Sakurai, T. (2019). The relationship between the gut microbiome and mild cognitive impairment in patients without dementia: a cross-sectional study conducted in Japan. Sci. Rep. 9, 19227.

Sanchez-Pinto, L.N., Venable, L.R., Fahrenbach, J., and Churpek, M.M. (2018). Comparison of variable selection methods for clinical predictive modeling. Int. J. Med. Inform. 116, 10–17.

Saravia, R., Ten-Blanco, M., Julià-Hernández, M., Gagliano, H., Andero, R., Armario, A., Maldonado, R., and Berrendero, F. (2019). Concomitant THC and stress adolescent exposure induces impaired fear extinction and related neurobiological changes in adulthood. Neuropharmacology 144, 345–357.

Sarkar, A., Harty, S., Lehto, S.M., Moeller, A.H., Dinan, T.G., Dunbar, R.I.M., Cryan, J.F., and Burnet, P.W.J. (2018). The Microbiome in Psychology and Cognitive Neuroscience. Trends Cogn. Sci. 22, 611–636.

Savignac, H.M., Tramullas, M., Kiely, B., Dinan, T.G., and Cryan, J.F. (2015). Bifidobacteria modulate cognitive processes in an anxious mouse strain. Behav. Brain Res. 287, 59–72.

Schmieder, R., and Edwards, R. (2011). Quality control and preprocessing of metagenomic datasets. Bioinformatics 27, 863–864.

Shi, L., Westerhuis, J.A., Rosén, J., Landberg, R., and Brunius, C. (2019). Variable selection and validation in multivariate modelling. Bioinformatics 35, 972–980.

Smith, A.D., Smith, S.M., de Jager, C.A., Whitbread, P., Johnston, C., Agacinski, G., Oulhaj, A., Bradley, K.M., Jacoby, R., and Refsum, H. (2010). Homocysteine-lowering by B vitamins slows the rate of accelerated brain atrophy in mild cognitive impairment: a randomized controlled trial. PLoS One 5, e12244.

Smith, C.J., Emge, J.R., Berzins, K., Lung, L., Khamishon, R., Shah, P., Rodrigues, D.M., Sousa, A.J., Reardon, C., Sherman, P.M., et al. (2014). Probiotics normalize the gut-brain-microbiota axis in immunodeficient mice. Am. J. Physiol. Gastrointest. Liver Physiol. 307, G793–G802.

Smyth, G.K. (2005). limma: Linear Models for Microarray Data. In Bioinformatics and Computational Biology Solutions Using R and Bioconductor (Springer-Verlag), pp. 397–420.

Snow, W.M., Stoesz, B.M., Kelly, D.M., and Albensi, B.C. (2014). Roles for NF-κB and gene targets of NF-κB in synaptic plasticity, memory, and navigation. Mol. Neurobiol. 49, 757–770.

Spitzer, R.L., Kroenke, K., and Williams, J.B. (1999). Validation and utility of a self-report version of PRIME-MD: the PHQ primary care study. Primary Care Evaluation of Mental Disorders. Patient Health Questionnaire. JAMA 282, 1737–1744.

Storey, J.D. (2002). A Direct Approach to False Discovery Rates. J. R. Stat. Soc. Ser. B. Stat. Methodol. 64, 479–498.

Strauss, E., Sherman, E.M.S., and Spreen, O. (2006). A Compendium of Neuropsychological Tests: Administration, Norms, and Commentary (Oxford University Press).

Sun, Y., Gooch, H., and Sah, P. (2020). Fear conditioning and the basolateral amygdala. F1000Res. 9, 53.

Švob Štrac, D., Pivac, N., and Mück-Šeler, D. (2016). The serotonergic system and cognitive function. Transl. Neurosci. 7, 35–49.

Tilg, H., Zmora, N., Adolph, T.E., and Elinav, E. (2020). The intestinal microbiota fuelling metabolic inflammation. Nat. Rev. Immunol. 20, 40–54.

Tillisch, K., Mayer, E.A., Gupta, A., Gill, Z., Brazeilles, R., Le Nevé, B., van Hylckama Vlieg, J.E.T., Guyonnet, D., Derrien, M., and Labus, J.S. (2017). Brain Structure and Response to Emotional Stimuli as Related to Gut Microbial Profiles in Healthy Women. Psychosom. Med. 79, 905–913.

Tzourio-Mazoyer, N., Landeau, B., Papathanassiou, D., Crivello, F., Etard, O., Delcroix, N., Mazoyer, B., and Joliot, M. (2002). Automated anatomical labeling of activations in SPM using a macroscopic anatomical parcellation of the MNI MRI single-subject brain. Neuroimage 15, 273–289.

van der Stelt, M., Mazzola, C., Esposito, G., Matias, I., Petrosino, S., De Filippis, D., Micale, V., Steardo, L., Drago, F., Iuvone, T., and Di Marzo, V. (2006). Endocannabinoids and β-amyloid-induced neurotoxicity in vivo: effect of pharmacological elevation of endocannabinoid levels. Cell. Mol. Life Sci. 63, 1410–1424.

Vioque, J., Navarrete-Muñoz, E.-M., Gimenez-Monzó, D., García-de-la-Hera, M., Granado, F., Young, I.S., Ramón, R., Ballester, F., Murcia, M., Rebagliato, M., and Iñiguez, C.; INMA-Valencia Cohort Study (2013). Reproducibility and validity of a food frequency questionnaire among pregnant women in a Mediterranean area. Nutr. J. 12, 26.

Wang, Q., Liu, D., Song, P., and Zou, M.H. (2015). Tryptophan-kynurenine pathway is dysregulated in inflammation, and immune activation. Front. Biosci. 20, 1116–1143.

Ward, Z.J., Bleich, S.N., Cradock, A.L., Barrett, J.L., Giles, C.M., Flax, C., Long, M.W., and Gortmaker, S.L. (2019). Projected U.S. state-level prevalence of adult obesity and severe obesity. N. Engl. J. Med. 381, 2440–2450.

Wechsler, D. (2012). WAIS-IV. Escala de inteligencia de Wechsler para adultos-IV. Manual técnico y de interpretación (NCS Pearson).

Wikoff, W.R., Pendyala, G., Siuzdak, G., and Fox, H.S. (2008). Metabolomic analysis of the cerebrospinal fluid reveals changes in phospholipase expression in the CNS of SIV-infected macaques. J. Clin. Invest. 118, 2661–2669.

Witt, E.D., and Goldman-Rakic, P.S. (1983). Intermittent thiamine deficiency in the rhesus monkey. II. Evidence for memory loss. Ann. Neurol. 13, 396–401.

Yang, Y., Shields, G.S., Wu, Q., Liu, Y., Chen, H., and Guo, C. (2020). The association between obesity and lower working memory is mediated by inflammation: Findings from a nationally representative dataset of U.S. adults. Brain Behav. Immun. 84, 173–179.

Yu, Q., McCall, D.M., Homayouni, R., Tang, L., Chen, Z., Schoff, D., Nishimura, M., Raz, S., and Ofen, N. (2018). Age-associated increase in mnemonic strategy use is linked to prefrontal cortex development. Neuroimage 181, 162–169.

STAR★METHODS

KEY RESOURCES TABLE

REAGENT or RESOURCE	SOURCE	IDENTIFIER
Biological Samples		
Human body fluids (feces, plasma)	This paper	N/A
Mice feces	This paper	N/A
Mice prefrontal cortex	This paper	N/A
Chemicals, Peptides, and Recombinant Proteins		
Methanol LC-MS	Scharlau	Cat#ME03262500
Lysing Matrix E	MP biomedicals	Cat#SKU116914050-CF
Acetic acid LC-MS	Scharlau	Cat#AC03470050
Critical Commercial Assays		
QIAamp DNA mini stool kit	QIAGEN	Cat#51504
Nextera DNA Flex Library Preparation kit	Illumina	Cat#20018705
TrueSeq stranded mRNA library preparation kit	Illumina	Cat#20020594
Truseq RNA Single Indexes	Illumina	Cat#20020492
Truseq RNA Single Indexes	Illumina	Cat#20020493
RNA 6000 Nano chip	Agilent	Cat#5067-1511
DNA 1000 chip	Agilent	Cat#5067-1504
KAPA Library Quantification Kit	Roche	Cat#07960204001
Deposited Data		
Metagenome Sequencing Data of Fecal Samples from Human subjects and Mice	European Nucleotide Archive (ENA)	Project number: PRJEB39631 Human samples accession numbers: ERS4859818-ERS4859933
Experimental Models: Organisms/Strains		
Mouse C57BL/6J	Charles River	N/A
Software and Algorithms		
SPSS software (version 19)	IBM	https://www.ibm.com/analytics/spss-statistics-software
Rstudio (version 1.3.959)	Rstudio Team	https://rstudio.com/
R (version 3.6)	R	https://www.r-project.org/
MATLAB (version R20217a)	Mathworks	https://www.mathworks.com/products/matlab.html
Statistical Parametric Mapping software (SPM12)	UCL Queen Square Institute of Neurology	https://www.fil.ion.ucl.ac.uk/spm/software/
MassHunter Data Analysis software	Agilent Technologies	https://www.agilent.com/en/products/software-informatics/mass-spectrometry-software
Prinseq-lite-0.20.4	(Schmieder and Edwards, 2011)	http://prinseq.sourceforge.net/
FLASh 1.2.11	(Magoč and Salzberg, 2011)	https://ccb.jhu.edu/software/FLASH/
Bowtie2-2.3.4.3	(Langmead and Salzberg, 2012)	http://bowtie-bio.sourceforge.net/bowtie2/index.shtml
MEGAHIT v1.1.2	(Li et al., 2015)	https://github.com/voutcn/megahit
Prodigal v2.6.342	(Hyatt et al., 2010)	https://github.com/hyattpd/Prodigal
HMMER	(Durbin et al., 1998)	http://hmmer.org/
Kaiju v1.6.2	(Menzel et al., 2016)	https://github.com/bioinformatics-centre/kaiju
STAR software (version 2.5.3a)	(Dobin et al., 2013)	https://github.com/alexdobin/STAR
Subread version (1.5.1)	(Liao et al., 2014)	http://subread.sourceforge.net/
Limma (version 3.30.13)	(Smyth, 2005)	https://bioconductor.org/packages/release/bioc/html/limma.html

(Continued on next page)

Continued

REAGENT or RESOURCE	SOURCE	IDENTIFIER
edgeR (version 3.26.8)	(Robinson et al., 2010)	https://bioconductor.org/packages/release/bioc/html/edgeR.html
DESeq2 (version 1.26.0)	(Love et al., 2014)	https://bioconductor.org/packages/release/bioc/html/DESeq2.html
ALDEx2 (version 1.18.0)	(Fernandes et al., 2014)	https://www.bioconductor.org/packages/release/bioc/html/ALDEx2.html
VITA (version 1.0.0)	(Janitza et al., 2018)	https://cran.r-project.org/web/packages/vita/index.html
Boruta (version 6.0.0)	(Kursa and Rudnicki, 2010)	https://cran.r-project.org/web/packages/Boruta/
Other		
1.5T Ingenia	Philips Healthcare	N/A
Dual energy X-ray absorptiometry	GE Healthcare	N/A
Cobas 8000 c702 analyzer	Roche Diagnostics	N/A
ADAM®A1c HA-8180V	ARKRAY, Inc	N/A
FastPrep-24™	MP biomedicals	N/A
Reversed-phase column (Zorbax SB-Aq 1.8 μm 2.1 × 50 mm)	Agilent Technologies	Cat#AG827700-914
Precolumn (Zorbax-SB-C8 Rapid Resolution Cartridge 2.1 × 30 mm 3.5 μm)	Agilent Technologies	Cat#AG873700-906
Shuttle chamber LE918	Panlab	N/A
Bioanalyzer 2100	Agilent	N/A
ABI 7900HT qPCR	Applied Biosystems	N/A
HiSeq 2500	Illumina	N/A
Qubit 3.0 fluorometer	Thermo Fisher Scientific	N/A
NextSeq 500	Illumina	N/A

RESOURCE AVAILABILITY

Lead Contact
Further information and requests for resources should be directed to and will be fulfilled by the Lead Contact José Manuel Fernández-Real (jmfreal@idibgi.org).

Materials Availability
This study did not generate new unique reagents.

Data and Code Availability
The data that support the findings of this study are available from the lead contact (jmfreal@idibgi.org) upon reasonable request. The accession numbers for the raw metagenomic sequence data of the 116 humans subjects reported in this paper are [European Nucleotide Archie]: ERS4859818-ERS4859933.

EXPERIMENTAL MODEL AND SUBJECT DETAILS

Clinical Study
Recruitment of Study Subjects
From January 2016 to October 2017, a cross-sectional case-control study was undertaken in the Endocrinology Department of Josep Trueta University Hospital. We included consecutive subjects with obesity (body mass index, BMI^{3}30kg/m^2) and age- and sex-matched nonobese subjects (BMI 18.5-<30kg/m^2), with an age range of 27.2-66.6 years. The sex Distribution and age range is reported in Table 1. All analysis were adjusted by gender to remove the influence of gender on the results. Exclusion criteria were: type 2 diabetes mellitus, chronic inflammatory systemic diseases, acute or chronic infections in the previous month; use of antibiotic, antifungal, antiviral or treatment with proton-pump inhibitors; severe disorders of eating behavior or major psychiatric antecedents; neurological diseases, history of trauma or injured brain, language disorders; and excessive alcohol intake (^{3} 40 g OH/day

in women or 80 g OH/day in men). The Institutional review board - Ethics Committee and the Committee for Clinical Research (CEIC) of Dr. Josep Trueta University Hospital (Girona, Spain) approved the study protocol and informed written consent was obtained from all participants.

Longitudinal Cohort
Cognitive tests and MRI variables were collected again in 93 consecutive subjects after 1 year of follow up. The sex distribution and age range is reported in Table 2. All analyses were adjusted by gender to remove the influence of gender on the results.

Animal Study
Male C57BL/6J mice (Charles River, France), weighing 23–26 g at the beginning of the experiment were used in this study. Mice were housed individually in controlled laboratory conditions with the temperature maintained at 21 ± 1°C, humidity at 55 ± 10%, and 7 h30/ 19 h30 light/dark cyles. All animals were fed a standard chow diet RM1 (Irradiated Vacuum packed, Dietex International Ltd.). The health status of each mouse included in the experimental schedule was checked every day before the experimental sessions and recorded in the experimenter protocol notebook. Health status checks included body weight, physical aspect, behavior, and clinical signs. No abnormalities were recorded in the animals included in this study. Animal procedures were conducted in strict accordance with the guidelines of the European Communities Directive 86/609/EEC regulating animal research and were approved by the local ethical committee (CEEA-PRBB). All the experiments were performed under blinded conditions (the researcher who administered the microbiota was blinded in relation to the memory scores of the subjects who provided the feces). Mice were given a cocktail of ampi- cillin and metronidazole, vancomycin (all at 500 mg/L), ciprofloxacin HCl (200 mg/L), imipenem (250 mg/L) once daily for 14 consec- utive days in drinking water, as previously described (Kelly et al., 2016). Seventy-two h later, animals were colonized via daily oral gavage of donor microbiota (150 μL) for 3 days. Animals were orally gavaged with saline (n = 11) and fecal material from healthy volunteers' samples from humans with better cognitive scores (n = 11) and humans with decreased cognitive scores (n = 11)). No differences were found related to BMI, age, years, sex within these two groups. To offset potential confounder and/or cage effects and to reinforce the donor microbiota phenotype, booster inoculations were given twice per week throughout the study. Animals were exposed to a series of behavioral testing including novel object recognition (NOR) test and fear conditioning with nociception assessed by the hot plate test to ensure specificity.

At the end of the study the animals were consecutively sacrificed. The cecum was removed, weighted and stored, and the feces collected and stored at −80°C for further microbiota analysis.

METHOD DETAILS

Clinical and Laboratory Parameters
Body composition was assessed using a dual energy X-ray absorptiometry (DEXA, GE lunar, Madison, Wisconsin). Fasting plasma glucose (FPG), lipids profile and high-sensitivity C-reactive protein (hsCRP) levels were measured using an analyzer (Cobas® 8000 c702, Roche Diagnostics, Basel, Switzerland). Glycated hemoglobin (HbA1c) was determined by performance liquid chromatog- raphy (ADAM®A1c HA-8180V, ARKRAY, Inc., Kyoto, Japan). *Dietary pattern:* The dietary characteristics of the subjects were collected in a personal interview using a validated food-frequency questionnaire (Vioque et al., 2013).

Magnetic Resonance Imaging (MRI)
MRI Acquisition and Image Pre-processing
All subjects were studied on a 1.5T Ingenia (Philips Healthcare, Best, the Netherlands) with eight channel head coils. Structural images were acquired using a 3D Turbo Field Echo Planar Imaging (TFEPI) sequence and parameters of echo time (TE) = 4.1ms, repetition time (TR) = 8.4ms, flip angle 8, field of view (FOV) 230x190 matrix. A total of 145 whole-brain images per subject with thickness axial slices of 1x1x1mm^3 with or without gap. The total scan time was 189.6 s. The anatomical imaging data was processed and analyzed using MATLAB version R2017a (The MathWorks Inc, Natick, Mass) and Statistical Parametric Mapping software (SPM12; The Welcome Department of Imaging Neuroscience, London). Preprocessing steps involved motion correction, spatial normalization and smoothing using a Gaussian filter (FWHM 8 mm). Data were normalized to Diffeomorphic Anatomical Regis- tration Through Exponentiated Lie (DARTEL) and resliced to a 2mm isotropic resolution in Montreal Neurological Institute (MNI) space.
Volumetric Brain Analyses
The Automated Anatomical Labeling (AAL) (Tzourio-Mazoyer et al., 2002) atlas was used to obtain the volumetric information of the right and left hippocampus, opercula (orbitalis, tringularis, opercularis), and middle and superior frontal gyri as informed by the involvement of these brain regions in verbal memory (Aslaksen et al., 2018; Colom et al., 2007; Gross et al., 2018; Yu et al., 2018) in 14394 participants. Volumetric differences for these targeted regions between participants with and without obesity were explored using independent sample t tests, and we used Pearson Partial correlations to explore for Each region was orthogonalized for sex, age and total gray matter volume in MATLAB version R2017a (The Math Works Inc, Natick, MA) and subsequently entered to SPSS to investigate associations between the gray matter volumes and the performance in the CVLT and the digit tasks controlling for age, sex, education, depressive symptoms, BMI and total intracranial volume in the whole sample, and within the obese and non-obese

groups. Finally, we investigated the associations and between the volume in the selected brain regions and the microbiota using Spearman correlation analyses corrected for multiple comparisons using q-values (Storey, 2002).

Neuropsychological Assessment in Humans
California Verbal Learning Test-II (CVLT)
CVLT is used to assess verbal learning and memory (Delis et al., 2000). It consists of 5 learning tests in which a list of words (list A) is presented and the subject is asked, immediately after each presentation, to recall as much words as possible. Then an interference list (list B) is presented, and the subject is asked to repeat the same task. CVLT Immediate Recall score is a result of the first five tests and provides information about the learning process. In the short delay test, the patient is asked to recall list A, free (CVLT Short Delayed Free Recall) or with semantic facilitation (CVLT Short Delayed Cued Recall). A higher score reflects a better memory function. About 30 min are necessary to administrate this test and its reliability ranges from 0.78-0.94 (Paolo et al., 1997).

Total Digit Span (TDS)
Working memory was assessed by the Digit Span, a subtest of the Wechsler Adult Intelligence Scale-III (WAIS-III) (Wechsler, 2012) a measure of general intellectual function. It is based on numbers and includes the Forward and Backward Digit Span tests. In the Forward Digit Span test, the examinee repeats a number sequence in the same order as presented. This constitutes a measure of working memory but also of attention. In the Backward Digit Span, the examinee repeats the number sequence in reverse order. Total Digit Span represents the total score of the two previous tests. A higher score reflects a better memory function. In a standardization sample of 394 participants (aged 16-89 years), the reliability coefficient was very high, ranging from 0.94-0.97 (Strauss et al., 2006).

The Patient Health Questionnaire-9 (PHQ-9)
Is a depression module of the PRIME-MD diagnostic instrument for mental disorders (Spitzer et al., 1999). It encompasses 9 items of depression symptoms plus a question about functional impairment and can be scored as a depression severity rating (scores of 10-14 moderate, 15-19 moderately severe and 20-27 severe depressive symptoms) or with an algorithm based on the DSM-IV criteria (major and minor episode). Scores of 10 or more have an 88% sensitivity and specificity. PHQ-9 score was considered as a possible confounding factor in the analyses.

Extraction of Fecal Genomic DNA and Whole-Genome Shotgun Sequencing
Total DNA was extracted from frozen human stools using the QIAamp DNA mini stool kit (QIAGEN, Courtaboeuf, France). Quantification of DNA was performed with a Qubit 3.0 fluorometer (Thermo Fisher Scientific, Carlsbad, CA, USA), and 1 ng of each sample (0.2 ng/μl) was used for shot gun library preparation for high-throughput sequencing, using the Nextera DNA Flex Library Prep kit (Illumina, Inc., San Diego, CA, USA) according to the manufacturers' protocol. Sequencing was carried out on a NextSeq 500 sequencing system (Illumina) with 2 X 150-bp paired-end chemistry, at the facilities of the Sequencing and Bioinformatic Service of the FISABIO (Valencia, Spain). The obtained input fastq files were decompressed, filtered and 3· ends-trimmed by quality, using prinseq-lite-0.20.4 program (Schmieder and Edwards, 2011) and overlapping pairs were joined using FLASH-1.2.11 (Magoč and Salzberg, 2011). Fastq files were then converted into fast files, and human and mouse host reads were removed by mapping the reads against the GRCh38.p11, reference human genome (Dec 2013), and GRCm38.p6, reference mouse genome (Sept 2017), respectively, by using bowtie2-2.3.4.3 (Langmead and Salzberg, 2012) with end-to-end and very sensitive options. Next, functional analyses were carried out by assembling the non-host reads into contigs by MEGAHIT v1.1.2 (Li et al., 2015) and mapping those reads against the contigs with bowtie2. Reads that did not assemble were appended to the contigs. Next, the program Prodigal v2.6.342 (Hyatt et al., 2010) was used for predicting codifying regions. Functional annotation was carried out with HMMER (Durbin et al., 1998) against the Kyoto Encyclopedia of Genes and Genomes (KEGG) database, version 2016 (Kanehisa and Goto, 2000) to obtain the functional subcategory, route and annotation of the genes. The filtering of the best annotations and the assignment of the orf annotation to every read were carried out using the statistical package R 3.1.0 (R Development Core Team, 2013) which also was used to count the aligned reads and to add the category and its coverage, and finally to build abundance matrices. Taxonomic annotation, was implemented with Kaiju v1.6.2 (Menzel et al., 2016) on the human and mouse-free reads. Addition of lineage information was added, counting of taxa and generation of an abundance matrix for all samples were performed using the package R (R Development Core Team, 2013). Fecal microbiota composition from mice was also analyzed following the same procedures as humans.

Metabolomics Analyses
For non-targeted metabolomics analysis, metabolites were extracted from fecal and plasma samples with methanol (containing phenylalanine-C13 as an internal standard) according to previously described methods (Wikoff et al., 2008). Briefly, for plasma samples 30μl of cold methanol were added to 10 μl of each sample, vortexed for 1 min and incubated for one h at -20°C. For faecal samples, the content of a 1.2 mL tube of Lysing Matrix E (MP biomedicals) and 600 μL of cold methanol were added to 10mg of sample. Samples were homogenized using FastPrep-24 (MP biomedicals) and were incubated overnight in a rocker at 4°C. Then, all samples were centrifuged for three minutes at 12,000 g, the supernatant was recovered and filtered with a 0.2 μm Eppendorf filter. Two μL of the extracted sample were applied onto a reversed-phase column (Zorbax SB-Aq 1.8 μm 2.1 $\times$ 50 mm; Agilent Technologies) equipped with a precolumn (Zorbax-SB-C8 Rapid Resolution Cartridge 2.1 $\times$ 30 mm 3.5 μm; Agilent Technologies)

with a column temperature of 60°C. The flow rate was 0.6 mL/min. Solvent A was composed of water containing 0.2% acetic acid and solvent B was composed of methanol 0.2% acetic acid. The gradient started at 2% B and increased to 98% B in 13 min and held at 98% B for 6 min. Post-time was established in 5 min.

Data were collected in positive and negative electrospray modes time of flight operated in full-scan mode at 50–3000 m/z in an extended dynamic range (2 GHz), using N2 as the nebulizer gas (5 L/min, 350°C). The capillary voltage was 3500 V with a scan rate of 1 scan/s. The ESI source used a separate nebulizer for the continuous, low-level (10 L/min) introduction of reference mass compounds 121.050873 and 922.009798, which were used for continuous, online mass calibration. MassHunter Data Analysis Software (Agilent Technologies, Barcelona, Spain) was used to collect the results, and MassHunter Qualitative Analysis Software (Agilent Technologies, Barcelona, Spain) to obtain the molecular features of the samples, representing different, co-migrating ionic species of a given molecular entity using the Molecular Feature Extractor algorithm (Agilent Technologies, Barcelona, Spain), as described 5,6. We selected samples with a minimum of 2 ions. Multiple charge states were forbidden. Compounds from different samples were aligned using a retention time window of 0.1% ± 0.25 min and a mass window of 20.0 ppm ± 2.0 mDa. We selected only those present in at least 50% of the samples of one group and corrected for individual bias.

Behavioral Testing in Mice

The NOR was performed in a V-maze as previously published (Burokas et al., 2014). Three phases of 9-min were performed on consecutive days. Mice were first habituated to the V-maze. On the second day, 2 identical objects (chess pieces) were presented to the mice, and the time that they spent exploring each object was recorded. In the test phase (3 h later for short-term memory or 24 h later for long-term memory), 1 of the familiar objects was replaced with a novel object (a different chess piece), and the time spent exploring each object (novel and familiar) was computed. A discrimination index was calculated as the difference between the times that the animal spent exploring the novel (Tn) and familiar (Tf) object divided by the total time of object exploration: (Tn-Tf)/(Tn + Tf).

Fear conditioning was conducted as described previously with some modifications (Burokas et al., 2017; Saravia et al., 2019). Mice were individually placed in a shuttle chamber (LE918, Panlab, Barcelona) surrounded by a sound-attenuating cabinet. The chamber floor was formed by parallel stainless-steel bars connected to a scrambled shock generator. On the training day, mice were habituated to the chamber during 180 s before the exposure to an acute beeping 30 s sound (80 dB). Each animal received an unconditioned stimulus (US) (0.6 mA footshock during 2 s) paired with the end of the sound (conditioned stimulus, CS). After the shock, the animal remained for 60 s in the shuttle chamber. To evaluate cued fear conditioning, mice were re-exposed to the CS in a novel environment (a wide white cylinder in the chamber) 24 h after the conditioning session. Mice were allowed to adapt for 180 s to the new environment which was followed by 30 s of the sound used in the training day. After the last sound trial, mice remained in the cylinder for 60 s. Fear memory was assessed as the percentage of time that mice spent freezing during the session. Freezing response, a rodent's natural response to fear, was evaluated by direct observation and defined as complete lack of movement, except for respiration for more than 1 s. The procedure was performed between 8.00 and 12.00 h in an experimental room different to the housing room.

Study of Gene Expression in Prefrontal Cortex
Sample Preparation
The mice brains were quickly removed and the medial prefrontal cortex was dissected according to the atlas of stereotaxic coordinates of mouse brain (Paxinos and Franklin, 1997). Brain tissues were then frozen by immersion in 2-methylbutane surrounded by dry ice, and stored at −80°C.
RNA Quality Control
Quality control of the RNA was performed using the RNA 6000 Nano chip (Agilent) on an Agilent Bioalyzer 2100 obtaining RIN values between 8.7 - 9.8.
RNA Libraries
Libraries were prepared from 500 ng of total RNA using the TruSeq stranded mRNA library preparation kit (Illumina, #20020594) with TruSeq RNA Single Indexes (Illumina, #20020492 and #20020493) according to the manufacturer's instruction reducing the RNA fragmentation time to 4.5 min. Prepared libraries were analyzed on a DNA 1000 chip on the Bioanalyzer and quantified using the KAPA Library Quantification Kit (Roche, #07960204001) on an ABI 7900HT qPCR instrument (Applied Biosystems). Sequencing was performed with 2x50 bp paired-end reads on a HiSeq 2500 (Illumina) using HiSeq v4 sequencing chemistry.
Bioinformatic Analysis
Raw sequencing reads in the fastq files were mapped with STAR version 2.5.3a (Dobin et al., 2013) to the Gencode release 17 based on the GRCm38.p6 reference genome and the corresponding GTF file. The table of counts was obtained with FeatureCounts function in the package subread, version 1.5.1. (Liao et al., 2014). The differential expression gene analysis (DEG) was assessed with voom+limma in the limma package version 3.30.13 (Smyth, 2005) and R version 3.4.3. Genes having less than 10 counts in at least 5 samples were excluded from the analysis. Raw library size differences between samples were treated with the weighted "trimmed mean method" TMM (Robinson and Oshlack, 2010) implemented in the edgeR package (Robinson et al., 2010). The normalized counts were used in order to make unsupervised analysis, PCA and clusters. For the differential expression (DE) analysis, read counts were converted to log2-counts-per-million (logCPM) and the mean-variance relationship was modeled with precision weights using voom approach in limma package.

QUANTIFICATION AND STATISTICAL ANALYSIS

First, normal distribution and homogeneity of variances were tested. Results are expressed as number and frequencies for categorical variables, mean and standard deviation (SD) for normal distributed continuous variables and median and interquartile range [IQ] for non-normal distributed continuous variables. To determine differences between study groups, we used χ^2 for categorical variables, unpaired Student's t test in normal quantitative and Mann-Whitney U test for non-normal quantitative variables. Spearman or Pearson analysis was used to determine the correlation between quantitative variables. Theses statistical analyses were performed with SPSS, version 19 (SPSS, Inc, Chicago, IL). Statistics can be found in the figures and legends.

Differential abundance analyses for taxa and functions associated to the memory tests and brain areas volumes were performed using the DESeq2 R package (Love et al., 2014), adjusting for age, body mass index, sex, education years, and Patient Health Questionnaire (PHQ)-9 scores. Fold change associated with a unit change in the corresponding test and adjusted *p-value*s are plotted for each taxon. Significantly different taxa are colored according to phylum. OTUs and bacterial functions were previously filtered so that only those with more than 10 reads in at least two samples were selected. To take into account the compositional structure of the microbiome data and rule out possible spurious associations microbiome data were also analyzed using a compositional approach with the ALDEx2 R package (Fernandes et al., 2014). ALDEx2 uses a Dirichlet-multinomial model to inter abundance from read counts. We used 128 Dirichlet Monte Carlo instances in the aldex.clr function, and then applied a generalized linear model with the aldex.glm function controlling for age, BMI, sex, education years and depression scores. The p values were then adjusted for multiple comparisons using q-values (Storey, 2002). We further analyzed the microbiome data adopting a multivariate machine learning feature selection strategy after transforming the data to take into account the compositional nature. Specifically, first we imputed the zero values with a Geometric Bayesian multiplicative replacement using the zcompositions R package. Then, we applied a clr transformation using the clr function from the compositions R package. Finally, we applied an all-relevant machine learning variable selection strategy to the clr-transformed data using the VITA algorithm (describe below).

Metabolomics data were also analyzed using machine learning (ML) methods. Omics datasets are usually composed of high-dimensional data with many redundant, non-informative and noisy features, i.e., not related to the outcome, with complex correlation patterns. Therefore, feature selection, plays a crucial role in omics data analysis. In this context, ML methods, such as random forest (RF), are promising computational approaches for feature selection in high-dimensional omics datasets. ML tree-based algorithms are particularly well-suited to this aim. Thus, variable selection tree-based methods have shown to perform better than classic regression-based methods in large datasets (Sanchez-Pinto et al., 2018).

When the main goal is building a predictive model, variable selection techniques designed to identify a minimal set of strongest predictors associated with the outcome are used (minimal-optimal problem). However, if the objective involves providing a more holistic pictures of the underlying mechanisms, networks and pathways involved in pathophysiological or metabolic processes, all-relevant variable selection methods, which include weak, correlated and redundant features, but avoid inclusion of uninformative variables, are preferred (Shi et al., 2019). Therefore, we adopted an all-relevant machine learning variable selection strategy applying two random forest-based methods, the Boruta algorithm (Kursa and Rudnicki, 2010) and the Variable Importance Testing Approach (VITA) method (Janitza et al., 2018). The Boruta and Vita approaches have been recently proposed as the two best-performing variable selection methods making use of RF for high-dimensional omics datasets (Degenhardt et al., 2019).

RF is an ensemble machine learning method based on "growing" many classification or regression trees. The advantage of the RF is that the observations not used for the construction of a specific tree (termed *out-of-bag* (OOB) observations) may be used to estimate the variable importance measure (VIM). Among the several VIMs, the permutation variable importance has shown to be the most reliable. However, a drawback of VIMs in RF is that they are not directly related to the statistical significance and there is no statistical test that discriminates between relevant and non-relevant features. Boruta and Vita are two RF-based approaches that deal with this issue. The **Boruta algorithm** is a wrapper algorithm that performs feature selection based on the learning performance of the model (Kursa and Rudnicki, 2010). The main idea behind this approach consists in: **a) Randomization.** Create a duplicate copy of the original features randomly permutate across the observations (the so-called shadow features) to remove their correlation with the response; **b) Model building.** Add the shadow feature to the original predictor feature dataset, built a RF with the extended dataset, and compute the normalized permutation importance (*Z*) scores for each predictor and shadow feature; **c) Statistical testing.** Find the maximum normalized importance among the shadow attributes (MZSA) and compare it with each original predictor feature using a Bonferroni corrected two-tailed binomial test. Predictor features with significantly higher, significantly lower, or non-significantly different *Z* scores than expected at random compared to the MZSA are deemed important, unimportant, or tentative, respectively. **d) Iteration**. Unimportant and shadow features are removed and the previous steps are repeated until the status of all features is decided or a predefined number of iterations has been performed. We run the Boruta algorithm with 500 iterations, a confidence level cut-off of 0.005 for the Bonferroni adjusted *p-value*s, 5000 trees to grow the forest (*ntree*), and a number of features randomly sampled at each split given by the rounded down number of features/3 (the *mtry* recommended for regression).

The **Vita algorithm** is based on the assumption that most variables in omics datasets are non-relevant for the biological question and can be used to approximate the unknown null distribution of variable importance scores to be able to select relevant variables based on *p-value*s (Janitza et al., 2018). First, the VIM for all features are obtained. The importance measure in the vita algorithm is not based on the "standard" permutation variable importance calculated using the OOB samples, but uses a strategy inspired in the cross-validation (CV) procedure, which is not based on the OOB observations, to obtain the CV permutation variable importance (CVPVI). The method randomly splits the data in a total of *k*-folds of equal size. For each *i*-fold, a RF is trained using all samples

that are not part of the *i*-test set, and the response variable is predicted for the samples in the *i*-test set. The procedure is repeated after permutating *n* times the values of the predictor variables. The permutation variable importance is calculated as the average difference in the prediction errors between the original data and the permutations, and the CVPVI is the average over all *k*-fold-specific permutation variable importance. Second, taking into account that for non-relevant features the change in accuracy is only due to random variations and thus it does not change (zero CVPVI) or slightly increases (negative CVPVI) when not using the variable for prediction, the non-positive CVPVI values are used compute the a symmetric null distribution of CVPVI scores around zero for non-relevant features by mirroring them on the y axis. From this approximated null distribution, *p-value*s can be calculated. As the null distribution is obtained from non-relevant features, this testing approach is only suitable for datasets with a large number of variables without effect. In our calculations we used 5000 trees, a 7-fold CV, and 10 permutations. *P*-values were then corrected using the Benjamini-Hochberg procedure for FDR.